Identification of a novel glucuronyltransferase from *Streptomyces chromofuscus* ATCC 49982 for natural product glucuronidation

Jie Ren • Caleb Don Barton • Kathryn Eternity Sorenson • Jixun Zhan

Department of Biological Engineering, Utah State University, 4105 Old Main Hill, Logan, UT 84322-4105, USA

Correspondence: Jixun Zhan

jixun.zhan@usu.edu

Abstract

Glycosylation is an effective way to increase the polarity of natural products. UDP-Glucuronyltransferases (UGTs) are commonly observed and extensively studied in phase II drug metabolism. However, UGTs in microorganisms are not well studied, which hampered the utilization of this type of enzyme in microbial glucuronidation of natural products. Screening of five actinomycete strains showed that *Streptomyces chromofuscus* ATCC 49982 can convert diverse plant polyphenols into more polar products, which were characterized as various glucuronides based on their spectral data. Analysis of the genome of this strain revealed a putative glucuronidation gene cluster that contains a UGT gene (*gcaC*) and two UDP-glucuronic acid biosynthetic genes (*gcaB* and *gcaD*). The *gcaC* gene was cloned and heterologously expressed in *Escherichia coli* BL21(DE3). Incubation of the purified enzyme with resveratrol and UDP-glucuronic acid led to the production of resveratrol-4'-O-β-D-glucuronide and resveratrol-3-O-β-D-glucuronide, allowing GcaC to be characterized as a flexible UGT. The optimal *in vitro* reaction pH and temperature for GcaC are 7.5 and 30 ℃, respectively. Its activity can be stimulated by Ca^{2+}, Mg^{2+} and Mn^{2+}, whereas Zn^{2+}, Cu^{2+} and Fe^{2+} showed inhibitory effects. Furthermore, GcaC has a broad substrate specificity, which can glucuronidate various substrates besides resveratrol, including quercetin, ferulic acid, vanillic acid, curcumin, vanillin, chrysin, zearalenone, and apigenin. The titers of resveratrol-4'-O-β-D-glucuronide and resveratrol-3-O-β-D-glucuronide in *E. coli*-GcaC were 78.381 ± 0.366 mg/L and 14.991 ± 0.248 mg/L from 114.125 mg/L resveratrol within 3 hours. Therefore, this work provides an effective way to produce

glucuronides of resveratrol and other health-benefitting natural products.

Key points

- A novel versatile microbial UDP-glucuronyltransferase was discovered and characterized from *Streptomyces chromofuscus* ATCC 49982.
- The UDP-glucuronyltransferase was expressed in *Escherichia coli* and can converts resveratrol into two glucuronides both *in vitro* and *in vivo*.
- The UDP-glucuronyltransferase has a highly flexible substrate specificity and is an effective tool to prepare mono- or diglucuronides of bioactive molecules.

Keywords *Streptomyces chromofuscus* · flexible substrate specificity · monoglucuronide · diglucuronide · microbial glucuronyltransferase

Introduction

Plant polyphenols are an important group of compounds with diverse chemical structures (Harborne and Baxter 1999; Tsao 2010). Stilbenoids and flavonoids are representative examples of polyphenols which are rich in commonly consumed fruits and vegetables, and both animal and human clinical studies showed their health-promoting effects and antioxidant characteristics (Rice-Evans 2001; Thilakarathna and Rupasinghe 2013). However, low water solubility and poor bioavailability often limits the beneficial effects of polyphenols. Introduction of polar groups such as sugar moieties into the structure is a widely used approach to improve the water solubility of bioactive molecules. As such, discovery of novel and versatile glycosyltransferases is important for adding new enzymes into the biocatalytic toolbox.

Sugar moieties often play important roles in binding of drugs to biological targets. They may also be involved in other biochemical processes such as distribution, metabolism, and excretion properties of drugs, which can affect the efficacy of its oral administration (Thorson et al. 2004; Weymouth-Wilson 1997; Yu et al. 2002). Glycosylated compounds often exhibit increased water-solubility, intestinal absorption, biological half-life, physicochemical stability and bioavailability for medical and cosmetic applications, while may also have lower toxicity compared to their aglycon forms (Bowles et al. 2005; Cai et al. 2013; Gachon et al. 2005; Imai et al. 2012; Kaminaga et al. 2003). Digitoxin, amphotericin, vancomycin, streptomycin, and daunomycin are some examples of the most biologically active natural products and commonly used therapeutics, with one or more sugar moieties (Pandey et al. 2014).

Sugar moieties can also contribute to other biological properties of natural products. For instance, the glucuronic acid moieties of glycyrrhizin are essential for its sweet taste (Chung et al. 2020).

Glycosyltransferases are the enzymes responsible for transferring sugar moieties from sugar donors to acceptors to yield corresponding glycosides. Microorganisms are a rich source of both natural products and natural product biosynthetic enzymes. Actinomycetes, the most ubiquitous group of gram-positive filamentous bacteria, are well characterized for their metabolic versatility (Nawani et al. 2013; Prakash et al. 2013). For example, they can decompose organic matter (such as cellulose) which is important for the carbon cycle and maintaining the soil structure (Kim 2016; Priyadharsini and Dhanasekaran 2015). In addition, actinomycetes can also produce various commercial products, such as pharmaceuticals (antibiotics, antitumor agents, etc) and nutraceuticals (Prakash et al. 2013; Remya and Vijayakumar 2008). Furthermore, many actinomycete genera produce industrially important enzymes applied in biotechnological applications and biomedical fields, such as amylases, cellulases, chitinases, xylanases, and proteases (Mehnaz et al. 2017; Nawani et al. 2013).

Glucuronidation is one of the common glycosylation reactions in nature. UDP-Glucuronyltransferases (UGTs) are the enzymes involved in glucuronidation, which are widely observed in metabolism of xenobiotics and endogenous components (bilirubin, bile acids, and certain hormones) during phase II metabolism, a common detoxification pathway in the human body (De Wildt et al. 1999; Wilkinson et al. 2008). There are mainly two phases for drug metabolism, namely functionalization reactions and

conjugation reactions. Glucuronidation is one of the phase II conjugation reactions. It was predicted that about 10% of the top 200 prescribed drugs recorded in USA are fully or partially metabolized by UGTs. UGTs transfer the glucuronic acid moiety from uridine 5'-diphosphoglucuronic acid (UDP-glucuronic acid) to various exogenous and endogenous compounds. They often work with cytochrome P450 enzymes (CYPs) to metabolize most hepatically cleared drugs.

Many fields such as drug development, sports drug testing, and the detection of agricultural residues often require the identification, quantification, and pharmacological evaluation of the glucuronidated metabolites (Wilkinson et al. 2011). However, chemical approaches like the Koenigs-Knorr reaction used for glucuronidation often suffer from poor yields and side reactions, as well as tedious protection-deprotection of the hydroxyl groups of sugar moieties (Engstrom et al. 2006; Stachulski et al. 2006). Enzymatic preparation of glucuronides represents a “green” alternative because of the selectivity, mild conditions and elimination of the need of toxic chemical reagents. Discovery of efficient and versatile UGTs is critical for the development of feasible and viable production process of glucuronides.

In our ongoing effort of discovering novel enzymes for natural product glycosylation, we found *Streptomyces chromofuscus* ATCC 49982 can convert resveratrol and several other natural products to corresponding glucuronides. We analyzed the genome of this strain and discovered a putative UGT gene flanked by two UDP-glucuronic acid biosynthetic genes. The UDP gene was then cloned and heterologously expressed in *Escherichia coli* BL21(DE3). The enzyme was

functionally characterized through *in vitro* reactions and its optimal reaction conditions were investigated. This enzyme is highly versatile and can convert a variety of substrates into monoglucuronides or diglucuronides. Therefore, this UGT represents a useful tool for the synthesis of glucuronidated metabolites. We also used the engineered *E. coli* strain to produce the two resveratrol glucuronides and the optimal bioconversion conditions were studied. In conclusion, the versatile UGT cloned and characterized from microorganism in this work lays the foundation for the microbial production of valuable glucuronides.

Materials and methods

General equipment and experimental materials

Agilent 1200 HPLC instrument with an Agilent Eclipse Plus-C_{18} column (5 μm, 250 mm × 4.6 mm) was used to analyze and purify the products. The samples were eluted with methanol-water (5:95 to 95:5 over 35 minutes, v/v, containing 0.1 % formic acid) at a flow rate of 1 mL/min. Low-resolution ESI-MS spectra were obtained on an Agilent 6130 single quadrupole LC-MS in the negative mode to confirm the molecular weights of glucuronides. All purified compounds were dissolved in in deuterated dimethyl sulfoxide (DMSO-d_6) to collect the NMR spectra on a Bruker Avance III HD Ascend-500 NMR instrument (500 MHz for ^{1}H NMR and 125 MHz for ^{13}C NMR). The chemical shift (δ) values are given in parts per million (ppm). The coupling constants (J values) are reported in hertz (Hz).

Phusion High-Fidelity DNA polymerase, restriction enzymes and T4 DNA ligase were purchased from New England Biolabs. PCR reactions were conducted with an

Arktik Thermal Cycler (Thermo Scientific). Genomic DNA extraction was performed using the Quick-DNA™ Fungal/Bacteria DNA Miniprep Kit (Zymo Research, USA). Plasmid extraction was performed using the Thermo Scientific GeneJET Plasmid Miniprep Kit (Thermo Scientific). Primers were ordered from Thermo Scientific and dissolved in Tris-EDTA (TE) buffer to the concentration of 100 ng/mL. Standard compounds like resveratrol, quercetin, curcumin, vanillic acid, ferulic acid, vanillin, chrysin, zearalenone, apigenin, resibufogenin, tetracycline were purchased from Sigma-Aldrich (USA). HisPur™ Ni-NTA resin, Luria-Bertani (LB) medium, yeast and malt extracts were purchased from Fisher Scientific (Rockford, IL, USA). Bradford assay solution was purchased from TCI America (Portland, OR, USA). Solvents and all other chemicals were purchased from Fisher Scientific. Milli-Q water was used throughout this study.

Strains, vectors, media, and culture conditions

Streptosporangium roseum No. 79089 (NRRL 2505) was provided by the ARS Culture Collection (NRRL) of the United States Department of Agriculture. *Streptomyces reseiscleroticus* ATCC 53903, *Actinomadura hibisca* P157-2 (ATCC 53557), and *S. chromofuscus* ATCC 49982 were obtained from the American Type Culture Collection (ATCC). *Streptomyces* sp. FERM BP-2474 was acquired from Patent and Bio-Resource Center, National Institute of Advanced Industrial Science and Technology, Japan.

E. coli XL1-Blue and BL21(DE3) were both purchased from Agilent. *E. coli* XL1-Blue was used for routine gene cloning and plasmid propagation. *E. coli* BL21(DE3) was used for protein expression and *in vivo* biotransformation. The pJET1.2 (Thermo

Fisher Scientific, USA) and pET28a (+) (Millipore Sigma, USA) vectors were used, respectively, to clone and express UGT. The *E. coli* strains were routinely grown at 37 °C on LB agar plates or in liquid LB medium (Fisher Scientific, USA). When necessary, carbenicillin (50 μg/mL) and kanamycin (50 μg/mL) were supplemented into the culture media for selecting correct clones. *S. chromofuscus* ATCC 49982 was grown on YM plate (4 g/L yeast extract, 10 g/L malt extract, 4 g/L glucose, and 20 g/L agar) or in YM broth (4 g/L yeast extract, 10 g/L malt extract, and 4 g/L glucose) at 28 °C. Recombinant UGT was expressed in *E. coli* BL21(DE3) at 28 °C. Isopropyl-1-thio-β-D-galactopyranoside (IPTG) (Gold Biotechnology, USA) was used at 200 μM to induce protein expression in *E. coli* BL21(DE3).

Screening of glucuronidating actinomycete strains

To test the ability of actinomyces to glucuronidate resveratrol, we screened five strains, namely, *S. roseum* No. 79089, *S. reseiscleroticus* ATCC 53903, *A. hibisca* ATCC 53557, *Streptomyces* sp. FERM BP-2474, and *S. chromofuscus* ATCC 49982. These bacteria were grown in 50 mL of YM medium in a rotary shaker at 250 rpm and 28 ℃ for 3 days.

Resveratrol (4 mg) was dissolved in DMSO and added into each culture. The cultures were incubated under the same conditions for an additional 4 days. After that, 1 mL of fermentation broth was sampled and centrifuged at 15,000 ×g for 10 min. The supernatant was analyzed by HPLC at 300 nm. In order to check whether *S. chromofuscus* ATCC 49982 can glucuronidate other substrates, quercetin, ferulic acid, and vanillic acid were incubated with the culture of this strain in a similar way. The

supernatant was analyzed by HPLC at 350 nm (quercetin) or 300 nm (ferulic acid and vanillic acid) using the same HPLC conditions for resveratrol.

Extraction and purification of compounds

To isolate the biotransformation products of resveratrol for structure elucidation, *S. chromofuscus* ATCC 49982 was cultivated in 1-L Erlenmeyer flasks, containing 250 mL of YM medium, to biotransform 20 mg of resveratrol. After 4 days, the fermentation broth was centrifuged at 4,000 ×g for 10 min. After water in the supernatant was evaporated, the residue was dissolved in 2 mL of methanol. The sample was subjected to Sephadex LH-20 column chromatography, and eluted with methanol-water (1:1, v/v). The products-containing fraction was further separated by reverse phase HPLC, and eluted with methanol-water (10-50%, 0-17 min; 50-95%, 17-22 min) containing 0.1% formic acid (v/v) to yield **1** (3.6 mg) and **2** (2.8 mg). Products **1** and **2** were also used to prepare a standard curve to quantify the formation of these products in the *in vitro* and *in vivo* reactions.

A similar procedure was used to isolate the biotransformation products of quercetin, ferulic acid and vanillic acid for structure elucidation except the HPLC methods for final compound purification. The gradient elution method with methanol-water (20-40%, 0-2 min; 40%, 2-15 min; 40-95%, 15-20 min) was used to yield product **3** (7.4 mg) and **4** (5.8 mg). The gradient elution method with methanol-water (5-60%, 0-15 min; 60-95%, 15-16 min; 95%, 16-18 min) was used to yield product **5** (4.8 mg), **6** (3.0 mg) and **7** (1.2 mg). All purified products were subjected to NMR analysis. The purified products were dissolved in DMSO-d_6. Their chemical structures were

221 characterized based on the NMR data (Supplementary Material).

222 **Genome analysis and amplification of the putative UGT gene from *S.***
223 ***chromofuscus* ATCC 49982**

224 The genomic DNA was extracted from *S. chromofuscus* ATCC 49982 using the Quick-
225 DNA™ Fungal/Bacterial Microprep Kit (Zymo Research, USA) by following the
226 manufacturer's standard procedure. The 454 next-generation sequencing system and
227 Rapid Annotation using Subsystem Technology (RAST) were used respectively to
228 sequence and annotate the genomic DNA of *S. chromofuscus*. The glucuronidation (*gca*)
229 gene cluster was deposited into GenBank under the accession number MZ666424. The
230 detailed functions of each gene in the gene cluster was predicted based on BLAST
231 analysis of the corresponding amino acid sequences.

232 Plasmids were extracted from *E. coli* via the GeneJET Plasmid Miniprep Kit
233 (Thermo Fisher Scientific). Primers were synthesized by Thermo Scientific (5'-
234 AATTGTTTAAACCATATGCGAGTACTGTTCACCAC-3' and 5'-AATTGCTAGCA
235 AGCTTTCAGACGATCTTCTGCAGGTC-3'). The primers (1 μM), genomic DNA
236 (0.2 μL), dNTP mix (200 μM), 5× buffer (4 μL), DMSO (0.4 μL), Phusion High-
237 Fidelity DNA Polymerase (0.2 μL at 2 U/μL) and nuclease-free water were mixed to
238 20 μL for amplification of the UGT (*gcaC*) gene (1,209 bp). The PCR program began
239 with an initial denaturation at 95 °C for 5 min, and then 20 cycles of touchdown
240 program (95 °C for 30 s, annealing at 70 °C for 40 s, decreasing 0.5 °C per cycle, and
241 extension at 72 °C for 100 s), followed by 20 cycles of regular program (95 °C for 30
242 s, annealing at 60 °C for 40 s, and extension at 72 °C for 100 s), and finally, 68 °C for

15 min of extension.

Construction of cloning and expression plasmids

After purification with a GeneJET Gel Extraction Kit, the target PCR product was ligated into the pJET1.2 cloning vector to yield pJR34 (pJET1.2-*gcaC*). After the pJR34 plasmid was confirmed by digestion check and sequencing using the Sanger method, the gene was excised from pJR34 and introduced to the pET28a expression vector between the *Nde*I and *Hin*dIII restriction sites to yield expression plasmid pJR36 (pET28a-*gcaC*). The ligation product was transferred into *E. coli* XL1-Blue competent cells through chemical transformation, and the transformants were selected on LB agar with 50 μg/mL kanamycin. The correct plasmids were confirmed by digestion check with *Nde*I and *Hin*dIII.

Heterologous expression of GcaC and *in vivo* biotransformation of resveratrol in *E. coli* BL21(DE3)

The expression plasmid pJR36 was transferred into *E. coli* BL21(DE3) through chemical transformation. The correct transformant of *E. coli* BL21(DE3)-pJR36 was picked from LB agar into 5 mL of LB medium supplemented with kanamycin (50 μg/mL), incubating at 37 °C with shaking (250 rpm) for about 12 hours. Then 500 μL of the seed culture was inoculated into 50 mL of LB broth with kanamycin (50 μg/mL) with shaking at 250 rpm and 37 °C. When the OD_{600} reached between 0.4 and 0.6, protein expression was induced with 200 μM IPTG, and the culture was maintained at 28 °C for an additional 16 hours with shaking at 250 rpm. After protein expression, 0.35 mM resveratrol and 0.11 M glucose were added as the substrates. The culture was

incubated under the same conditions for an additional 48 hours. After fermentation, 1 mL of the culture was sampled and centrifuged at 15,000 ×g for 10 min. 100 μL of the supernatant was subjected to analysis on HPLC (at 300 nm).

Functional characterization of GcaC through *in vitro* enzymatic reactions

GcaC was purified as described in Supplementary Material. We characterized the function of GcaC by reacting the enzyme with the substrate resveratrol. Enzymatic assays were conducted in a 100-μL reaction system, which included 20 mM Tris-HCl (pH 8.0), 2.2 mM substrate, 1 mM $MgCl_2$, 2 mM sugar donor (UDP-glucuronic acid), and 23.7 μg purified recombinant GcaC protein. The mixtures were thoroughly mixed and incubated at 30 ℃ for 6 hours, and then 200 μL of HPLC-grade methanol was added to terminate the reaction. The reaction mixtures were centrifuged at 13,000 ×g for 10 min, and supernatants were collected to analyze the products by LC-MS.

The substrate specificity of GcaC was investigated using additional sugar-acceptor substrates, including curcumin, quercetin, ferulic acid, vanillic acid, vanillin, chrysin, apigenin, zearalenone, tetracycline and resibufogenin. In terms of sugar-donor substrates, another structurally similar sugar-donor substrate UDP-glucose was also reacted with resveratrol, besides UDP-glucuronic acid. Reaction products were analyzed by LC-MS after centrifugation.

Determination of the optimal *in vitro* reaction conditions

Purified resveratrol glucuronides were used to establish standard curves for quantifying product formation. The effects of reaction temperature, pH and metal ions on the catalytic activity of GcaC were examined. To determine the optimum temperature, the

reaction mixtures with resveratrol as the substrate were incubated at different temperatures (20, 25, 30, 35, 40, 45, and 50 °C) for 6 hours. Glucuronidation reactions were conducted as described before except with 1.0 mM resveratrol. In order to find out the optimum pH, GcaC was reacted with resveratrol at 30 °C in 200 mM phosphate buffer with different pH values (pH 4.5, 5.5, 6.0, 6.5, 7.0, 7.5, 8.0, 8.5, and 9.0). The conversion rate of resveratrol was quantified by HPLC. Control reaction was conducted under the same conditions, but without GcaC. Different metal ions such as $CaCl_2$, $CuCl_2$, $FeSO_4$, $MgCl_2$, $MnCl_2$, and $ZnCl_2$ were also tested. Control reaction was performed under the same conditions without adding these metal ions. The experiments were carried out with individually divalent metal ion at the final concentration of 10 mM, and UDP-glucuronic acid and resveratrol were used as sugar donor and sugar acceptor, respectively. All reactions were performed in triplicate and conversion rates were expressed as the mean ± standard deviation.

Whole-cell bioconversion of resveratrol into resveratrol glucuronides by *E. coli* BL21(DE3)-pJR36

E. coli BL21(DE3)-pJR16 was grown and induced as described above. The cells were collected by centrifugation for whole-cell bioconversion after IPTG induction at 28 °C for 16 hours. Phosphate buffer was used to re-suspend the cells, and cell density was determined using a UV-Vis spectrophotometer (Thermo Scientific, Rockford, USA) by recording the OD_{600} value. In order to determine the whole-cell bioconversion conditions, different pH values (pH 4.5, 5.5, 6.0, 6.5, 7.0, 7.5, and 8.5), temperatures (25, 30, 35, 40, and 45 °C), cell densities (OD_{600} 2.5, 5, 7.5, 10, 12.5, and 15), reaction

times (1, 2, 3, 4, and 5 h) and substrate concentrations (0.25, 0.5, 1.0, 1.5, 2.0 and 2.5 mM) were investigated. Product formation was quantified by HPLC. Finally, the whole-cell biotransformation experiment was performed in a 1-L reaction system under the optimal conditions. The reaction consisted of *E. coli* BL21(DE3)-pJR36 cells (OD_{600} 10.0) and 0.5 mM resveratrol, and the bioconversion process was performed at 40 °C, pH 6.5, and 250 rpm for 3 hours.

Results

Screening of different actinomycete strains for the ability to glycosylate resveratrol

Actinomyctes are known to produce a variety of bioactive natural products and contain abundant biosynthetic enzymes. We hypothesized that some of these strains may have versatile UGTs that can introduce the glucuronic acid moiety to plant polyphenols such as resveratrol. To this end, resveratrol was incubated with five different strains, including *S. roseum* No. 79089, *S. reseiscleroticus* ATCC 53903, A. *hibisca* P157-2, *Streptomyces* sp. FERM BP-2474, and *S. chromofuscus* ATCC 49982. HPLC analysis revealed that two more polar metabolites, at 15.5 min for product **1** and 17.0 min for product **2** respectively, were synthesized from resveratrol by *S. chromofuscus* ATCC 49982 (Fig. 1a). The UV absorption patterns of the products were both similar to that of resveratrol, suggesting that these two polar products are derivatives of the substrate (Fig. 1b). However, no products were detected in the other four strains.

Characterization of the two biotransformed products of resveratrol by *S. chromofuscus* ATCC 49982

ESI-MS spectra of both **1** (Fig. 1d) and **2** (Fig. 1e) showed the same corresponding quasimolecular ions $[M-H]^-$ at *m/z* 402.8 and $[2M-H]^-$ at *m/z* 806.7, respectively. Therefore, products **1** and **2** have the same molecular weight of 404, which is 176 mass units larger than the substrate resveratrol, suggesting that a glucuronic acid moiety was added to different hydroxyl groups of resveratrol.

In order to elucidate the chemical structures, two purified products **1** and **2** were subjected to NMR analysis (Figures S1-S10). The ^{13}C NMR spectra of **1** (Figure S2) and **2** (Figure S7) both revealed 20 carbon signals. In addition to the 14 signals belonging to resveratrol, six additional carbon signals at δ_C 170.5, 100.3, 76.2, 75.9, 73.4, and 71.8 for **1** and δ_C 170.1, 100.5, 77.2, 75.8, 72.9, and 71.4 for **2** were found in the spectra, further suggesting that a sugar moiety was added to resveratrol at one of its hydroxyl groups. Unlike glucose and other common sugars, this sugar moiety has a carbon signal at around δ_C 170, indicating the presence of a carboxyl group. Both the ^1H and ^{13}C signals of this sugar moiety supported the presence of a glucuronic acid moiety. As shown in the ^1H NMR spectra (Figures S1 and S6), the anomeric proton signals at δ_H 5.07 (d, J = 7.5 Hz), and 4.99 (d, J = 7.7 Hz) of **1** and **2**, respectively, indicated the β-configuration of these two compounds for the glucuronic acid moiety. HMBC spectrum of **1** revealed the correlation of H-1" at δ_H 5.07 to C-4' at δ_C 156.9 (Figures 2 and S5), which confirmed that **1** has a glucuronic acid moiety at C-4'. Similarly, H-1" at δ_H 4.99 of **2** had HMBC correlation to C-3 at δ_C 158.4, indicating that the glucuronic acid moiety was introduced at C-3 (Figures 2 and S10). Therefore, products **1** and **2** were characterized as resveratrol-4'-O-β-D-glucuronide and

353 resveratrol-3-O-β-D-glucuronide, respectively. The NMR data of **1** and **2** are consistent
354 with those reported in literature (Wang et al. 2004).

355 **Characterization of the biotransformed products of quercetin, ferulic acid and**
356 **vanillic acid by *S. chromofuscus* ATCC 49982**

357 To check whether *S. chromofuscus* can also glucuronidate other natural products,
358 quercetin, ferulic acid and vanillic acid were incubated with *S. chromofuscus*
359 respectively. We found that all these three substrates can be glucuronidated into one or
360 two glucuronides (Fig. 3).

361 When quercetin was used as substrate, HPLC analysis (Fig. 3a) showed that two
362 polar products at 16.1 and 18.8 min, respectively, were formed from quercetin. Two
363 products showed the similar UV spectra (Figures S11a and S11b) to the substrate. ESI-
364 MS spectra (Figures S12a and S12b) of both **3** and **4** showed the corresponding quasi-
365 molecular ion $[M-H]^-$ at *m/z* 476.9 and 476.6, respectively. Therefore, products **3** and **4**
366 have the same molecular weight of 478, which is 176 mass units larger than the
367 substrate quercetin, indicating that a glucuronic acid moiety was added to different
368 hydroxyl groups of quercetin.

369 When ferulic acid was used as the substrate, a polar product **5** at 12.8 min was
370 detected by HPLC (Fig. 3b). Two more polar products **6** and **7** appeared at 9.7 and 10.8
371 min when vanillic acid was incubated with *S. chromofuscus* ATCC 49982 (Fig. 3c).
372 These products showed the similar UV spectra (Figures S11c-e) to the corresponding
373 substrates. The ESI-MS spectra (Figures S12c-e) of **5**-**7** showed a $[M-H]^-$ ion peak at
374 *m/z* 368.9, 342.9, and 342.9, respectively, indicating that their molecular weights are

370, 344 and 344 Da, which are consistent with the addition of a glucuronic acid moiety to the substrates ferulic acid and vanillic acid. Therefore, *S. chromofuscus* was found to be able to glucuronidate various phenolic natural products.

The NMR spectra of products **3**-**7** were collected (Figures S13-S37). The ^{13}C NMR spectra (Figures S14 and S19) of compounds **3** and **4** both showed 21 carbon signals. In addition to the signals from quercetin, six additional carbon signals at δ_C 170.1, 99.1, 75.6, 75.4, 72.8, and 71.2 for **3** and δ_C 169.7, 101.0, 76.0, 75.8, 73.8, and 71.3 for **4** were found in the spectra. These signals were similar to those from the glucuronic acid moiety of **1** and **2**, thus suggesting that a glucuronic acid moiety was added to one of the hydroxyl groups in quercetin. As shown in the ^{1}H NMR spectra (Figures S13 and S18), the anomeric proton signals at δ_H 5.29 (d, J = 7.3 Hz), and 5.50 (d, J = 7.5 Hz) of **3** and **4**, respectively, indicated the β-configuration of the sugar moiety in these two compounds. HMBC spectrum of **3** revealed the correlation of H-1" at δ_H 5.29 to C-7 at δ_C 162.2 (Figures 2 and S17), which confirmed that **3** has a glucuronic acid moiety at C-7. Similarly, H-1" of **4** at δ_H 5.50 had HMBC correlation to C-3 at δ_C 133.0, indicating that the glucuronic acid moiety was introduced at C-3 (Figures 2 and S22). Therefore, products **3** and **4** were characterized as quercetin-7-O-β-D-glucuronide and quercetin-3-O-β-D-glucuronide, respectively. The NMR data of **3** and **4** are consistent with those reported in literature (Marvalin and Azerad 2011a).

The ^{13}C NMR spectrum of compounds **5** revealed 16 carbon signals. Compared to the substrate ferulic acid, there were six additional carbon signals at δ_C 170.2, 99.2, 76.1, 75.3, 72.9, and 71.4, further suggesting that a glucuronic acid moiety was added

to ferulic acid. As shown in the ^{1}H NMR spectrum (Figure S23), the anomeric proton signal of **5** at δ_H 5.13 (d, J = 7.1 Hz) indicated the β-configuration of the glucuronic acid moiety. HMBC spectrum of **5** revealed the correlation of H-1" (δ_H 5.13, d, J = 7.1 Hz) to C-4 at δ_C 147.8 (Figures 2 and S27), which confirmed that the position of glucuronic acid moiety is at C-4 of **5**. Therefore, **5** was characterized as ferulic acid-4-O-β-D-glucuronide. The NMR data were assigned based on the 1D and 2D NMR spectra for the first time.

The ^{13}C NMR spectra of both **6** (Figure S29) and **7** (Figure S34) showed 14 carbon signals. In addition to the eight carbon signals from vanillic acid, six additional carbon signals at δ_C 170.8, 99.2, 76.4, 74.7, 72.9, and 71.6 were observed for **6** and δ_C 170.4, 94.6, 75.9, 75.7, 72.3, and 71.6 for **7**, indicating that a glucuronic acid moiety was added to vanillic acid at different positions to yield the two products. As shown in the ^{1}H NMR spectra (Figures S28 and S33), the anomeric proton signals of **6** and **7** at δ_H 5.11 (d, J = 6.1 Hz) and 5.54 (d, J = 7.5 Hz), respectively, indicated the β-configuration of the glucuronic acid moiety in these compounds. HMBC spectrum of **6** revealed the correlation of H-1" at δ_H 5.11 to C-4 at δ_C 150.0 (Figures 2 and S32), which confirmed that **6** has a glucuronic acid moiety at C-4. Similarly, H-1" of **7** at δ_H 5.54 had HMBC correlation to C-7 at δ_C 164.4, indicating that the glucuronic acid moiety was introduced at C-7 (Figures 2 and S37). Therefore, **6** and **7** were characterized as vanillic acid-4-O-β-D-glucuronide and vanillic acid-7-O-β-D-glucuronide, respectively. The NMR data of compound **6** is consistent with those reported in literature (Almeida et al. 2017) and the NMR data of compound **7** were assigned based on the 1D and 2D NMR spectra for

the first time.

Discovery of a putative glucuronidation gene cluster from *S. chromofuscus* ATCC 49982

To find out which enzyme is responsible for the glucuronidation in *S. chromofuscus* ATCC 49982, we analyzed the genome of this strain that was previously sequenced by our group. Annotation of the genome indicated that there are more than 30 glycosyltransferases in *S. chromofuscu* ATCC 49982. To narrow down, we looked at the genes adjacent to these glycosyltransferase genes. A gene cluster (Fig. 4a) putatively involved in the glucuronidation was discovered, and the predicted functions of the genes are shown in Table 1. The five genes, named *gcaA-E*, were predicted to be TetR transcriptional regulator, UDP-glucose dehydrogenase, UDP-glucuronosyltransferase, UDP-glucose pyrophosphorylase, and MFS transporter, respectively. While *gcaA* and g*caE* might be involved in the regulation of the gene cluster and sugar transport, respectively, *gcaB*, *gcaC* and *gcaD* were proposed to be involved in the biosynthesis and transfer of UDP-glucuronic acid (Fig. 4b). More specifically, GcaD (containing 320 amino acids or aa) generates UDP-glucose from glucose-1-phosphate as a UDP-glucose pyrophosphorylase, GcaB (484 aa) functions as a UDP-glucose dehydrogenase to synthesize UDP-glucuronic acid, and finally GcaC (402 aa) transfers the UDP-glucuronic acid moiety to a sugar acceptor such as resveratrol.

BLAST analysis of the amino acid sequence of GcaC revealed that it is homologous to a number of glycosyltransferases including a few uncharacterized UDP-

glucuronyl/UDP-glucosyltransferase, such as those from *Streptomyces malaysiensis* (GenBank accession number NIY63294.1, 408 aa, 70% identity) and *Streptomyces violaceusniger* (GenBank accession number AEM85024.1, 404 aa, 68% identity). Although both genes are not functionally characterized so far, they still provide useful information to predict the function of GcaC.

Heterologous expression and purification of GcaC from *E. coli* BL21(DE3)

To identify the function of GcaC, we amplified this gene from the genomic DNA of *S. chromofuscus*, and ligated it to pET28a to yield the corresponding expression plasmid, pJR36 (pET28a-*gcaC*). The plasmid was then expressed in *E. coli* BL21(DE3) with IPTG induction. Ni-NTA column chromatography was used to purify the N-His_6-tagged GcaC from the cell lysate and the purified enzyme was analyzed by SDS-PAGE. As shown in Fig. 5a, GcaC (~43.4 kDa) was expressed and purified from *E. coli* BL21(DE3)-pJR36 to homogeneity and the isolation yield of this enzyme was 11.87 mg/L.

***In vitro* functional characterization of GcaC**

To check the function of purified GcaC, resveratrol was incubated with this enzyme in the presence of UDP-glucuronic acid. HPLC analysis showed that compared to the control (trace i, Fig. 5b), two polar products were formed from resveratrol (trace ii, Fig. 5b). Two products showed the similar UV spectra to the substrates. ESI-MS spectra (Figs. 5c and 5d) of these products showed the corresponding quasi-molecular ion $[M-H]^-$ at *m/z* 402.9, respectively. Therefore, they have the same molecular weight of 404, which is 176 mass units larger than the substrate resveratrol, indicating that a glucuronic

463 acid moiety was added to different positions of resveratrol. Furthermore, the retention
464 times of these two *in vitro* products were the same as those of resveratrol-4'-O-β-D-
465 glucuronide and resveratrol-3-O-β-D-glucuronide produced in the *in vivo*
466 biotransformation by *S. chromofuscus*. Formation of the two resveratrol glucuronides
467 in the *in vitro* reactions allowed the characterization of GcaC as the responsible UGT
468 in *S. chromofuscus*.

469 **Broad substrate specificity of GcaC toward sugar acceptor substrates**

470 To explore the substrate specificity of GcaC, this enzyme was reacted with different
471 sugar donors and sugar acceptors. UDP-Glucose is structurally similar to UDP-
472 glucuronic acid and the BLAST analysis of the sequence of GcaC suggested that this
473 enzyme is homologous to a predicted UDP-glucuronyltransferase or UDP-
474 glucosyltransferase from *S. malaysiensis* (Table 1). Therefore, we reacted resveratrol
475 with UDP-glucose in the presence of GcaC. However, no products were formed from
476 resveratrol (data not shown), indicating that GcaC is a specific UDP-
477 glucuronyltransferase that strictly transfers UDP-glucuronic acid.

478 We next investigated the substrate specificity of GcaC to sugar acceptor substrates
479 by reacting it with various natural products, including quercetin, ferulic acid, vanillic
480 acid, curcumin, vanillin, chrysin, zearalenone and apigenin, with UDP-glucuronic acid
481 in the presence of GcaC. When quercetin was used as the substrate, HPLC analysis (Fig.
482 6a) showed that six polar products were formed. All products showed the similar UV
483 spectra (Figures S38a-f) to the substrate. ESI-MS spectra (Figures S39a-f) of **Q1**-**Q6**
484 showed the corresponding quasi-molecular ion $[M-H]^-$ at *m/z* 653.0, 653.0, 476.9, 476.9,

476.9, and 476.9, respectively. Therefore, products **Q3-Q6** have the same molecular weight of 478, which is 176 mass units larger than the substrate quercetin, indicating that a glucuronic acid moiety was added to different hydroxyl groups of quercetin. Since quercetin has five free phenolic hydroxyl groups, we propose that the glucuronic acid moiety was introduced to four of these hydroxyl groups to generate the four monoglucuronides. Among these monoglucuronides, **Q3** and **Q4** had the same retention times as products **3** and **4**, which were characterized as quercetin-7-O-β-D-glucuronide and quercetin-3-O-β-D-glucuronide, respectively. The molecular weight of both **Q1** and **Q2** were found to be 654, which is 352 mass units larger than the substrate quercetin or 176 units larger than products **Q3-Q6**, suggesting that two glucuronic acid moieties were added to quercetin to form diglucuronides. Therefore, this enzyme not only adds the glucuronic acid moiety to different hydroxyl groups of quercetin, but also accepts the resulting monoglucuronides as the substrates to further generate diglucuronides.

When ferulic acid was incubated with GcaC, one polar product **F1** at 12.8 min was detected by HPLC (Fig. 6b). Similarly, one product **VA1** appeared at 9.7 min when vanillic acid was used as a sugar acceptor (Fig. 6c). Both products showed the similar UV spectra (Figures S38g and S38h) to the corresponding substrates. The ESI-MS spectra (Figures S39g and S39h) of **F1** and **VA1** showed a $[M-H]^-$ ion peak at *m/z* 368.9 and 342.9, respectively, indicating that their molecular weights are 370 Da and 344 Da, which are consistent with the addition of a glucuronic acid moiety to ferulic acid and vanillic acid, respectively. Furthermore, the retention times of **F1** and **VA1** are the same as **5** and **6** from the biotransformation by *S. chromofuscus* 49982, namely ferulic acid-

4-O-β-D-glucuronide and vanillic acid-4-O-β-D-glucuronide.

Meanwhile, when curcumin was used as the substrate, HPLC analysis showed that compared to the negative control (trace i, Fig. 6d), GcaC generated two polar products **C1** and **C2** (trace ii, Fig. 8d), at 21.8 and 25.3 min respectively. The two products had the UV spectra (Figures S38i and S38j) similar to that of the substrate. The ESI-MS spectra (Figures S39i and S39j) of the two products showed the $[M-H]^-$ ion peak at *m/z* 719.1 and 542.8, indicating that their molecular weights are 720 Da and 544 Da, respectively. These are consistent with a diglucuronide and a monoglucuronide of curcumin, whose molecular weight is 368 Da. This result further indicated that GcaC can transfer one or two glucuronic acid moieties to curcumin.

Similarly, we also used vanillin as the substrate, and one polar product **VN1** at 10.0 min was detected by HPLC (Fig. 6e). One product **CS1** was also observed at 22.0 min when chrysin was incubated with GcaC (Fig. 6f). Both products showed the similar UV spectra (Figures S38k and S38l) to their relative substrates. The ESI-MS spectra (Figures S39k and S39l) of **VN1** and **CS1** showed a $[M-H]^-$ ion peak at *m/z* 326.9 and 428.8, respectively, indicating that their molecular weights are 328 Da and 430 Da, which are consistent with the addition of a glucuronic acid moiety to vanillin and chrysin, respectively. Similarly, when zearalenone and apigenin were used as the substrates, HPLC analysis showed that compared to the negative controls (trace i, Figures 6g and 6h), GcaC generated a product **Z1** (trace ii, Fig. 6g) at 23.0 min from zearalenone and a product **A1** (trace ii, Fig. 6h) at 19.0 min from apigenin. The products showed the UV spectra (Figures S38m and S38n) similar to those of their substrates.

529 The ESI-MS spectrum (Figure S39m) of **Z1** exhibited the $[M-H]^-$ ion peak at *m/z* 493.1,
530 which means the molecular weight is 494 Da and it is in accord with the addition of a
531 glucuronic acid moiety to zearalenone with a molecular weight of 318. The ESI-MS
532 spectrum (Figure S39n) of **A1** showed the $[M-H]^-$ ion peak at *m/z* 445.1, indicating that
533 molecular weight is 446 Da. This is consistent with a monoglucuronide of apigenin,
534 whose molecular weight is 270 Da. Therefore, GcaC synthesized the corresponding
535 glucuronides from zearalenone and apigenin.

536 Other substrates, including tetracycline and resibufogenin, were also reacted with
537 UDP-glucuronic acid in the presence of GcaC. However, no products were detected by
538 HPLC (data not shown).

539 **Determination of the optimal *in vitro* reaction conditions of GcaC**

540 The effects of reaction temperature and pH on the GcaC-catalyzed glucuronidation
541 were examined. Purified GcaC was incubated with resveratrol and UDP-glucuronic
542 acid under different conditions. First, the reaction was conducted at different
543 temperatures ranging from 20 °C to 50 °C. The conversion rates of resveratrol were
544 quantified by HPLC and compared. As shown in Fig. 7a, GcaC has the highest
545 glucuronidation activity at 30 °C with the highest conversion rate. When the
546 temperature increased from 20 °C to 30 °C, the conversion rate of resveratrol increased
547 from 29.61% to 70.85%. However, when the reaction temperatures were above 30 °C,
548 the resveratrol conversion rate gradually decreased. Therefore, the optimum reaction
549 temperature for GcaC was determined to be 30 °C.

550 Next, we determined the pH effect on the glucuronidation activity of GcaC. The

enzyme was reacted with resveratrol in 200 mM phosphate buffer at 30 °C but at different pH values, including 4.5, 5.5, 6, 6.5, 7, 7.5, 8, 8.5 and 9. With the increase of pH from 4.5 to 7.5, the conversion rate of resveratrol by GcaC steadily increased from 7.8% to 59.3%. Nevertheless, when the pH value further increased to 9.0, the conversion rate decreased to 37.2% (Fig. 7b). Hence, the optimum pH for GcaC is 7.5.

Apart from temperature and pH effects, we also investigated the effect of various metal ions on the activity of GcaC. At 10 mM, we found that Ca^{2+}, Mg^{2+}, and Mn^{2+} had a simulative function on the UGT activity of GcaC (Fig. 7c). With these three metal ions applied in the enzymatic reaction, the catalytic activity was 1.33, 1.27, and 1.09-fold higher than that of the control group, respectively. Among these three metal ions, Ca^{2+} has the strongest stimulating effect. By contrast, the activity of GcaC was inhibited when Cu^{2+}, Fe^{2+}, and Zn^{2+} were added into the reaction system. The conversion rate of resveratrol decreased from 52.3% to 39.1%, 48.6%, and 43.8% (Fig. 7c), respectively. In conclusion, the optimal *in vitro* reaction conditions for purified GcaC are at 30 °C, pH 7.5 with 10 mM of Ca^{2+}.

Optimized production of resveratrol-4'-O-β-D-glucuronide and resveratrol-3-O-β-D-glucuronide with the engineered *E. coli* BL21(DE3)

We next tested whether *E. coli* BL21(DE3)-pJR36 can convert resveratrol into the two glucuronides. To this end, resveratrol was incubated with the IPTG-induced broth of this engineered strain, with *E. coli* BL21(DE3)-pET28a as the negative control. As shown in Fig. 8a, compared to the commercial standard (trace i) and negative control (trace ii), incubation of resveratrol with *E. coli* BL21(DE3)-pJR36 yielded the

573 glucuronidation products **1** and **2**.

574 *In vivo* biotransformation of resveratrol by *E. coli* BL21(DE3)-pJR36 indicated that
575 GcaC can generate resveratrol-4'-O-β-D-glucuronide as the major product from
576 resveratrol in *E. coli*, which provides an alternative approach to biosynthesize this
577 resveratrol glucuronide. Therefore, it is critical to discover the optimal conditions for
578 this whole-cell bioconversion process. The effect of different cell concentrations on the
579 formation of resveratrol glucuronides at 40 °C overnight was first investigated, ranging
580 from OD_{600} 2.5 to 15.0. In the presence of 1.5 mM resveratrol and 0.11 M glucose, we
581 discovered that the conversion rate of resveratrol steadily increased with increasing cell
582 concentrations within the range of OD_{600} 2.5-10.0 (Fig. 8b). The conversion rate of
583 resveratrol in the biotransformation system reached 53.8% when the OD_{600} value was
584 10.0, which was 27.3% higher than the titer at OD_{600} 2.5. However, further increase in
585 cell concentration resulted in a drop of the conversion rate, indicating that oversaturated
586 cells did not yield more products.

587 The conversion of resveratrol to its glucuronides was also determined by HPLC at
588 different pH values (pH 4.5-8.5). When the reaction pH was 6.5, the conversion rate
589 reached its highest level, namely 38.1% (Fig. 8c), which is 23.2% higher than that at
590 pH 4.5. We next investigated the impact of temperature on the whole-cell conversion
591 efficiency of resveratrol to its glucuronides. Specifically, *E. coli* BL21(DE3)-pJR36
592 cells (OD_{600} 10.0) were incubated with resveratrol at different temperatures ranging
593 from 25 to 45 °C in 200 mM phosphate buffer (pH 6.5). It was clearly proved that the
594 higher temperature could effectively improve the conversion of resveratrol into

595 resveratrol-4'-O-β-D-glucuronide and resveratrol-3-O-β-D-glucuronide. The highest
596 conversion rate reached 48.6% at 40 °C (Fig. 8d).

597 To determine how the bioconversion time affects the conversion rate of resveratrol
598 in the engineered *E. coli* strain, we conducted a time course analysis for the conversion
599 of 1.0 mM resveratrol to its glucuronides. The experiments were performed with GcaC-
600 expressing *E. coli* BL21(DE3) strain (OD_{600} 10.0) at 40 °C in 200 mM phosphate buffer
601 (pH 6.5). The reaction was sampled at 1, 2, 3, 4 and 5 hours. Within the first 3 hours,
602 the conversion rate of resveratrol increased from 18.0% to 34.8% (Fig. 8e). After that,
603 the increase in the conversion rate slowed down gradually. Thus, we chose 3 hours as
604 the preferred reaction time.

605 Substrate concentration can also affect the bioconversion rate. Therefore, we next
606 tested different resveratrol concentrations ranging from 0.25 to 2.5 mM, for further
607 optimizing the production of resveratrol-4'-O-β-D-glucuronide and resveratrol-3-O-β-
608 D-glucuronide. The reactions were conducted at pH 6.5, OD_{600} 10, and 40 °C for 3
609 hours. The conversion rates of resveratrol to its glucuronides were similar when the
610 substrate concentration were 0.25 mM and 0.5 mM, namely 82.6 % to 83.2%. However,
611 the conversion rate fell to 41.7% when the concentration of resveratrol was further
612 increased to 1.0 mM (Fig. 8f). As a result, 0.5 mM was deemed to be the optimal
613 substrate concentration according to the productivity of resveratrol glucuronides under
614 the selected reaction conditions.

615 Finally, we scaled up the reaction to 1 L considering all the effects mentioned above.
616 The titers of resveratrol-4'-O-β-D-glucuronide and resveratrol-3-O-β-D-glucuronide

were 0.194 ± 0.001 mM (equivalent to 78.381 ± 0.366 mg/L) and 0.037 ± 0.001 mM (equivalent to 14.991 ± 0.248 mg/L) from a total of 0.5 mM (equivalent to 114.125 mg/L) of resveratrol in 3 hours at 40 ℃ in 200 mM phosphate buffer (pH 6.5) with shaking at 250 rpm.

Discussion

Polyphenols, such as resveratrol, quercetin and curcumin from certain foods and dietary supplements, have promising biological activities. (Sauer and Plauth 2017). However, their health benefits in the human body are often limited due to poor water solubility. Glycosylation is an effective approach to improve the water solubility and bioavailability (Ren et al. 2022). Actinomycetes are well-known for their ability to biosynthesize novel and pharmaceutically relevant secondary metabolites with various bioactivities (Fidan et al. 2019). Among them, *Streptomyces* is widely used to produce industrially important bioactive molecules, such as streptomycin, avermictin and oxytetracycline. *S. chromofuscus* ATCC 49982 is a typical example which produces the anti-cholesterol polyketide natural product herboxidiene (Yu et al. 2013). In this study, five actinomycete strains were screened for the ability to biotransform resveratrol, and only *S. chromofuscus* ATCC 49982 was found to generate two glycosides, which were structurally characterized as resveratrol-3-O-β-D-glucuronide and resveratrol-4'-O-β-D-glucuronide, respectively. Resveratrol is a plant-derived stilbenoid with a variety of bioactivities, including antimicrobial, antiviral, anti-inflammatory, antioxidant, antiaging, anticancer, antiplatelet, phytoestrogenic, neuro-protective, and cardio-protective activities (Thuan et al. 2018; Yu et al. 2002). Its ubiquitous presence in diets

639 such as grapes, wine, olive oil, white tea, peanuts and cranberries has attracted
640 considerable research interest (Pervaiz 2003; Wang et al. 2002). Nevertheless, its low
641 bioavailability results in limited absorption after oral administration and impedes the
642 formulation of functional foods. Furthermore, its sensitivity to air and light also hinders
643 the nutraceutical and medicinal applications and exploitation of resveratrol (Francioso
644 et al. 2014; Jeon et al. 2016; Uesugi et al. 2017).

645 Resveratroloside (resveratrol-4'-O-β-glucoside) and polydatin (resveratrol-3-O-β-
646 glucoside) are two common water-soluble derivatives of resveratrol, and they exhibit
647 anticancer and antioxidant activities. Moreover, they can prevent coronary heart
648 diseases (Shimoda et al. 2013). In the meantime, resveratroloside and polydatin are
649 more resistant to enzymatic oxidation than resveratrol (King et al. 2006). In other words,
650 glycosylation of resveratrol can extend its half-life in the cell and maintains the
651 beneficial antioxidant capacity and biological properties (Regev-Shoshani et al. 2003).
652 As one of the most abundant forms of resveratrol in nature, polydatin is the major
653 bioactive compound of *Polygonum cuspidatum* root which is used to treat cardiac
654 ailments, including atherosclerosis and inflammation in Japanese and Chinese folk
655 medicine (Romero-Pérez et al. 1999). While the two resveratrol glucuronides obtained
656 in this work are structurally slightly different than the glucosides, it will be interesting
657 to find out how these molecules perform *in vivo*. In fact, resveratrol-3-O-β-D-
658 glucuronide and resveratrol-4'-O-β-D-glucuronide were previously reported to be the
659 metabolites of resveratrol in the human body. While resveratrol has cytotoxicity to
660 human peripheral blood mononuclear cells at 30 μM, these glucuronides did not show

any cytotoxicity at 300 μM. The ubiquitous human β-glucuronidase can convert the metabolites back to resveratrol locally or systematically *in vivo* (Wang et al. 2004). Therefore, the two resveratrol glucuronides may represent useful pro-drugs of resveratrol for clinical applications.

S. chromofuscus ATCC 49982 was also found to be able to glucuronidate other phenolic compounds, indicating that the dedicated UGT in this strain is flexible and can transfer the glucuronic acid moiety to different positions of phenolic compounds. Interestingly, vanillic acid-4-O-β-D-glucuronide and vanillic acid-7-O-β-D-glucuronide were synthesized when vanillic acid is used as the substrate. The production of vanillic acid-7-O-β-D-glucuronide is somewhat surprising as the sugar moiety was introduced to the carboxyl group, which is quite chemically different than the phenolic hydroxyl group, further indicating that the UGT in *S. chromofuscus* ATCC 49982 is a highly versatile enzyme. Encouraged by the high flexibility of this enzyme, we sought to find and identify the dedicated the UGT in *S. chromofuscus* ATCC 49982. We were able to spot the most possible glycosyltransferase gene responsible for the observed glucuronidation in this strain because that it is flanked by two UDP-glucuronic acid biosynthetic genes (*gcaD* and *gcaB*). This gene was cloned and expressed in *E. coli* BL21(DE3). The purified GcaC was functionally characterized as a versitile UGT, providing a reference enzyme for future investigatin of more microbial UGTs.

UGTs play important roles in plant growth and development. They can also be a useful tool for structural modification of bioactive molecules in metabolic engineering

683 applications, because it can greatly change the bioactivity, solubility, or stability of
684 metabolites (De Bruyn et al. 2015; Kren and Martínková 2001). For example, the
685 sweetness and solubility were greatly improved from glycyrrhetinic acid to its final
686 product glycyrrhizin through two steps of glucuronidation, which is used as an anti-
687 hepatitis agent and a sweetener worldwide (Xu et al. 2016). In fact, the two glucuronic
688 acid moieties of glycyrrhizin also reduce the side-effects (Yonekura and Hanada 2011).
689 Researchers found that glucuronidated anthocyanins showed improved color stability
690 in response to light compared to its glucosylated form, indicating that UGTs may be
691 used to stabilize natural colorants for industrial use, such as commercial food colorant
692 products (Osmani et al. 2009). Glucuronidation can also improve the bioactivity of
693 natural products. For instance, glucuronidated flavonoids exhibited relatively stronger
694 inhibitory activity of amyloid β (Aβ) and human islet amyloid polypeptide (hIAPP)
695 aggregation than their aglycons (Hmidene et al. 2017). More importantly, the
696 conjugation location of glucuronidation can alter the biological effects. Morphine-6-
697 glucuronide is a much more potent agonist than morphine itself, while morphine-3-
698 glucuronide is an extremely potent antagonist (Paul et al. 1989; Smith et al. 1990). This
699 finding indicates that glucuronides may have very distinctive effects themselves.
700 To explore the pential of GcaC as a useful biocatalytic tool, we investigated the
701 substrate specificity of this enzyme. Although *in vitro* reaction results revealed that
702 GcaC is a specific UDP-glucuronyltransferase, it showed high flexibilty toward the
703 sugar acceptor substrates. A varitey of substrates, such as quercetin, ferulic acid, vanillic
704 acid, curcumin, vanillin, chrysin, zearalenone and apigenin, can be accepted by GcaC

as sugar acceptors to yield various glucuronides. Compared to BpUGAT from plant red daisy (*Bellis perennis*) that is specific for anthocyanin glucuronidation (Sawada et al. 2005), GcaC showed relaxed substrate specificity to sugar acceptors. Interestingly, it was found that different products may be produced from the same substrates in the *in vivo* biotransformation by *S. chromofuscus* ATCC 49982 and *in vitro* reactions with purified GcaC, likely due to the availability of UDP-glucuronic acid and other factors in the cells. For example, quercetin-7-O-β-D-glucuronide and quercetin-3-O-β-D-glucuronide were obtained as the major products when quercetin was incubated with *S. chromofuscus* ATCC 49982. However, a total of six glucuronides were detected *in vitro* when quercetin was reacted with UDP-glucuronic acid in the presence of purified GcaC. Interestingly, among the six products, four monoglucuronides and two diglucuronides of quercetin were obtained based on LC-MS analysis. Similarly, *in vitro* reaction of GcaC with curcumin also yielded a monoglucuronide and a diglucuronide. These results indicated that GcaC is a highly versatile enzyme for the synthesis of glucuronides. Compared to the tedious chemical methods to synthesize glucuronides (Sharipova et al. 2017), discovery of GcaC provides an effective tool to prepare various glucuronides from different phenolic compounds in an environmental-friendly and efficient way.

The optimal *in vitro* enzymatic reactions and *in vivo* bioconversion conditions of GcaC were investigated in this work. The optimum reaction temperature and pH for this enzyme were found to be 7.5 and 30 °C in phosphate buffer, which are both slightly lower than BpUGAT from *B. perennis* (8.0 and 35 °C). However, these two UGTs have

727 different response to metal ions. For example, Ca^{2+} had an inhibitory effect on BpUGAT,
728 but stimulated the activity of GcaC. Similarly, Mg^{2+} and Mn^{2+}, with negligible effects
729 on the catalytic activity of BpUGAT (Sawada et al. 2005), enhanced the activity of
730 GcaC. By contrast, the inhibitory effects of Cu^{2+}, Zn^{2+} and Fe^{2+} on GcaC is similar to
731 the previous discovered UBGAT from *Scutellaria baicalensis* (Nagashima et al. 2000).
732 Generally, UGTs fulfill key metabolic functions in various organisms, and
733 microbial UGTs are not well studied compared to those in mammalian systems. In the
734 human body, the activity of UGTs can modify the lipid phase fluidity of the microsomal
735 membrane, which is critical for its physiological function (Zakim and Vessey 1974).
736 Mammalian UGTs play an important role in the elimination of xenobiotics and
737 lipophilic compounds from the body, and the native acceptor substrates could be
738 bilirubin, hormones, bile acids, retinoids, and thyroid hormones (Clarke et al. 1991;
739 Radominska-Pandya et al. 1999). GcaC is a microbial UGT. Based on the BLAST
740 analysis and enzymatic studies, we propose that the native function of GcaC is a UDP-
741 glucuronyltransferase and might have the following potential functions: (1) GcaC
742 contributes to the cell surface polysaccharide biosynthesis. Specifically, it may transfer
743 sugars from intracellular nucleotide sugars to the lipid carrier acceptor in cytoplasmic
744 membrane and then synthesize the long-chain polysaccharides such as
745 exopolysaccharides, which are produced by many bacteria and excreted into the
746 environment during growth (Li et al. 2010); (2) GcaC uses native peptidyl nucleosides
747 as acceptor substrates, such as cytosine, to biosynthesize endogenous peptide-
748 nucleoside antibiotics for defensing themselves from other bacteria or fungi (Gould and

749 Guo 1994); (3) GcaC may catalyze the glucuronidation of lipophilic endogenous
750 metabolites and xenobiotics, like some fungal UGTs, and may play a role in the
751 degradation of carcinogenic pollutants in their surrounding environment. Additional
752 work is required to identify the exact function of GcaC in *S. chromofuscus* ATCC 49982
753 (Bezalel et al. 1997; Wackett and Gibson 1982).

754 Even though some glucuronyltransferases have been found in the microorganisms,
755 many of them require association with another enzyme to display the function (Tracy
756 et al. 2007; Sugiura et al. 2010). Moreover, their functions are almost limited to the
757 synthesis of saccharides (DeAngelis and White 2002; Wang et al. 2018; Wang et al.
758 2020). By contrast, GcaC represents a novel UGT from microorganism with broad
759 substrate specificity and can glucuronylate various plant polyphenols. BLAST analysis
760 showed that this microbial UGT showed little or no homology to UGTs from other
761 sources. For example, GcaC has less than 25% identity to BpUGAT from *B. perennis*
762 (Gene bank accession number AB190262) (Sawada et al. 2005), GuUGAT from
763 *Glycyrrhiza uralensis* (Gene bank accession number KT759000) (Xu et al. 2016), and
764 UBGAT from *Scutellaria baicalensis* (Gene bank accession number BAC98300)
765 (Nagashima et al. 2000). Discovery and characterization of GcaC yielded a reference
766 enzyme for future identification of additional UGTs from microorganisms. More
767 importantly, this highly flexible enzyme may (1) glucuronidate a variety of substrates,
768 (2) introduce the glucuronic acid moiety to different positions of a substrate, and (3)
769 introduce one or two glucuronic acid moieties to a substrate to yield monoglucosides
770 and diglucosides. Therefore, *S. chromofuscus* ATCC 49982, GcaC and *E. coli*

BL21(DE3)-GcaC can be used to prepare desired glucuronides from particular substrates. For example, vanillic acid-COOH-glucuronide was only previously detected in human urine after tea intake, and it was only identified by using MS analysis without available NMR data (Ridder et al. 2012; van der Hooft et al. 2012). This work for the first time biosynthesized vanillic acid-7-O-β-D-glucuronide for complete structure elucidation. This work also demonstrated that this novel UGT can be efficiently expressed in *E. coli* BL21(DE3) and the engineered strain can be used as a whole-cell biocatalyst to prepare resveratrol glucuronoides. The titers of resveratrol-4'-O-β-D-glucuronide and resveratrol-3-O-β-D-glucuronide were 78.381 ± 0.366 mg/L and 14.991 ± 0.248 mg/L from 114.125 mg/L resveratrol in a 1-L reaction system within 3 hours. Overall, this work provides a highly versatile UGT that can serve as a useful biocatalyst to prepare valuable glucuronides of bioactive molecules.

Author contributions JR and JZ conceived and designed research. JR, CB, and KS conducted experiments. JR and JZ analyzed data. JR, CB, KS and JZ wrote the manuscript. All authors read and approved the manuscript.

Funding information This work was supported by the National Science Foundation Award CBET-2044558. The Bruker Avance III HD Ascend-500 NMR instrument used in this research was funded by the National Science Foundation Award CHE-1429195.

Compliance with ethical standards

Conflict of interest The authors declare that they have no conflict of interest.

Ethical approval This article does not contain any studies with human participants

or animals performed by any of the authors.

Data availability statement All data generated or analyzed during this study are included in this published article (and its supplementary information files).

References

Almeida AF, Santos CuN, Ventura MR (2017) Synthesis of new sulfated and glucuronated metabolites of dietary phenolic compounds identified in human biological samples. J Agric Food Chem 65(31):6460–6466. https://doi.org/10.1021/acs.jafc.6b05629

Bezalel L, Hadar Y, Cerniglia CE (1997) Enzymatic mechanisms involved in phenanthrene degradation by the white rot fungus *Pleurotus ostreatus*. Appl Environ Microbiol 63(7):2495–2501. https://doi.org/10.1128/aem.63.7.2495-2501.1997

Bowles D, Isayenkova J, Lim E-K, Poppenberger B (2005) Glycosyltransferases: managers of small molecules. Curr Opin Plant Biol 8(3):254–263. https://doi.org/10.1016/j.pbi.2005.03.007

Briggs B, Baker P, Belvo M, Black T, Getman B, Kemp C, Muth W, Perun T, Strobel Jr R, Paschal J (1999) Microbial process for preparation of glucuronides of raloxifene. J Ind Microbiol Biot 23(3):194–197. https://doi.org/10.1038/sj.jim.2900716

Cai Z, Huang J, Luo H, Lei X, Yang Z, Mai Y, Liu Z (2013) Role of glucose transporters in the intestinal absorption of gastrodin, a highly water-soluble drug with good oral bioavailability. J Drug Target 21(6):574–580.

https://doi.org/10.3109/1061186X.2013.778263

Cassinelli G, Ballabio M, Grein A, Merli S, Rivola G, Arcamone F, Barbieri B, Bordoni T (1987) A new class of biosynthetic anthracyclines: anthracyclinone glucuronides. J Antibiot 40(7):1071–1074. https://doi.org/10.7164/antibiotics.40.1071

Chung SY, Seki H, Fujisawa Y, Shimoda Y, Hiraga S, Nomura Y, Saito K, Ishimoto M, Muranaka T (2020) A cellulose synthase-derived enzyme catalyses 3-O-glucuronosylation in saponin biosynthesis. Nat Commun 11(1):1–11. https://doi.org/10.1038/s41467-020-19399-0

Clarke DJ, George SG, Burchell B (1991) Glucuronidation in fish. Aquat Toxicol 20(1-2):35–56. https://doi.org/10.1016/0166-445X(91)90040-G

De Bruyn F, Maertens J, Beauprez J, Soetaert W, De Mey M (2015) Biotechnological advances in UDP-sugar based glycosylation of small molecules. Biotechnol Adv 33(2):288–302. https://doi.org/10.1016/j.biotechadv.2015.02.005

De Wildt SN, Kearns GL, Leeder JS, van den Anker JN (1999) Glucuronidation in humans. Clin Pharmacokinet 36(6):439–452. https://doi.org/10.2165/00003088-199936060-00005

DeAngelis PL, White CL (2002) Identification and molecular cloning of a heparosan synthase from *Pasteurella multocida* type D. J Biol Chem 277(9):7209–7213. https://doi.org/10.1074/jbc.M112130200

Engstrom KM, Daanen JF, Wagaw S, Stewart AO (2006) Gram scale synthesis of the glucuronide metabolite of ABT–724. J Org Chem 71(22):8378-8383.

837 https://doi.org/10.1021/jo0611972
838 Fidan O, Yan R, Zhu D, Zhan J (2019) Improved production of antifungal angucycline
839 Sch47554 by manipulating three regulatory genes in *Streptomyces sp.* SCC-
840 2136. Appl Biochem Biotechnol 66(4):517–526.
841 https://doi.org/10.1002/bab.1748
842 Francioso A, Mastromarino P, Restignoli R, Boffi A, d'Erme M, Mosca L (2014)
843 Improved stability of trans-resveratrol in aqueous solutions by
844 carboxymethylated (1,3/1,6)-β-D-glucan. J Agric Food Chem 62(7):1520–1525.
845 https://doi.org/10.1021/jf404155e
846 Gachon CM, Langlois-Meurinne M, Saindrenan P (2005) Plant secondary metabolism
847 glycosyltransferases: the emerging functional analysis. Trends Plant Sci
848 10(11):542–549. https://doi.org/10.1016/j.tplants.2005.09.007
849 Gould S, Guo J (1994) Cytosylglucuronic acid synthase (cytosine: UDP-
850 glucuronosyltransferase) from *Streptomyces griseochromogenes*, the first
851 prokaryotic UDP-glucuronosyltransferase. J Bacteriol 176(5):1282–1286.
852 https://doi.org/10.1128/jb.176.5.1282-1286.1994
853 Harborne JB, Baxter H (1999) The handbook of natural flavonoids. Volume 1 and
854 Volume 2. John Wiley and Sons.
855 Hmidene AB, Hanaki M, Murakami K, Irie K, Isoda H, Shigemori H (2017) Inhibitory
856 activities of antioxidant flavonoids from *Tamarix gallica* on amyloid
857 aggregation related to Alzheimer's and type 2 diabetes diseases. Biol Pharm Bull
858 40(2):238–241. https://doi.org/10.1248/bpb.b16-00801

859 Imai H, Kitagawa M, Ishihara K, Masuoka N, Shimoda K, Nakajima N, Hamada H
860 (2012) Glycosylation of *trans*-resveratrol by plant-cultured cells. Biosci
861 Biotech Bioch 76(8):1552–1554. https://doi.org/10.1271/bbb.120126
862 Jeon YO, Lee J-S, Lee HG (2016) Improving solubility, stability, and cellular uptake of
863 resveratrol by nanoencapsulation with chitosan and γ-poly (glutamic acid).
864 Colloids Surf B 147:224–233. https://doi.org/10.1016/j.colsurfb.2016.07.062
865 Kaminaga Y, Nagatsu A, Akiyama T, Sugimoto N, Yamazaki T, Maitani T, Mizukami
866 H (2003) Production of unnatural glucosides of curcumin with drastically
867 enhanced water solubility by cell suspension cultures of *Catharanthus roseus*.
868 FEBS Lett 555(2):311–316. https://doi.org/10.1016/S0014-5793(03)01265-1
869 Kim S-K (2016) Marine Enzymes Biotechnology: Production and Industrial
870 Applications, Part II-Marine Organisms Producing Enzymes, Volume 79, 1st
871 edition. Academic Press.
872 King RE, Bomser JA, Min DB (2006) Bioactivity of resveratrol. Compr Rev Food Sci
873 F 5(3):65–70. https://doi.org/10.1111/j.1541-4337.2006.00001.x
874 Kren V, Martínková L (2001) Glycosides in medicine: "The role of glycosidic residue
875 in biological activity". Curr Med Chem 8(11):1303–1328.
876 https://doi.org/10.2174/0929867013372193
877 Li X, Wang L, Bai L, Yao C, Zhang Y, Zhang R, Li Y (2010) Cloning and
878 characterization of a glucosyltransferase and a rhamnosyltransferase from
879 *Streptomyces* sp. 139. J Appl Microbiol 108(5):1544–1551.
880 https://doi.org/10.1111/j.1365-2672.2009.04550.x

881 Li Y, Baldauf S, Lim E-K, Bowles DJ (2001) Phylogenetic analysis of the UDP-
882 glycosyltransferase multigene family of *Arabidopsis thaliana*. J Biol Chem
883 276(6):4338–4343. https://doi.org/10.1074/jbc.M007447200
884 Marvalin C, Azerad R (2011a) Microbial glucuronidation of polyphenols. J Mol Catal
885 B Enzym 73(1-4):43–52. https://doi.org/10.1016/j.molcatb.2011.07.015
886 Marvalin C, Azerad R (2011b) Microbial production of phase I and phase II metabolites
887 of propranolol. Xenobiotica 41(3):175–186.
888 https://doi.org/10.3109/00498254.2010.535219
889 Mehnaz D, Abdulla K, Aiysha D, Zaheer A, Mukhtar S (2017) Actinomycetes: a source
890 of industrially important enzymes. J Proteom Bioinform 10:12
891 https://doi.org/10.4172/JPB.1000456
892 Nagashima S, Hirotani M, Yoshikawa T (2000) Purification and characterization of
893 UDP-glucuronate: baicalein 7-O-glucuronosyltransferase from *Scutellaria*
894 *baicalensis* Georgi. cell suspension cultures. Phytochemistry 53(5):533–538.
895 https://doi.org/10.1016/S0031-9422(99)00593-2
896 Nawani N, Aigle B, Mandal A, Bodas M, Ghorbel S, Prakash D (2013) Actinomycetes:
897 Role in biotechnology and medicine. BioMed Res Int 2013: 687190.
898 https://doi.org/10.1155/2013/687190
899 Osmani SA, Halkjær Hansen E, Malien-Aubert C, Olsen C-E, Bak S, Lindberg Møller
900 B (2009) Effect of glucuronosylation on anthocyanin color stability. J Agric
901 Food Chem 57(8):3149–3155. https://doi.org/10.1021/jf8034435
902 Pandey RP, Parajuli P, Shin JY, Lee J, Lee S, Hong Y-S, Park YI, Kim JS, Sohng JK

(2014) Enzymatic biosynthesis of novel resveratrol glucoside and glycoside derivatives. Appl Environ Microbiol 80(23):7235–7243. https://doi.org/10.1128/AEM.02076-14

Paul D, Standifer KM, Inturrisi CE, Pasternak G (1989) Pharmacological characterization of morphine-6 β-glucuronide, a very potent morphine metabolite. J Pharmacol Exp Ther 251(2):477-483.

Pervaiz S (2003) Resveratrol: from grapevines to mammalian biology. FASEB J 17(14):1975–1985. https://doi.org/10.1096/fj.03-0168rev

Prakash D, Nawani N, Prakash M, Bodas M, Mandal A, Khetmalas M, Kapadnis B (2013) Actinomycetes: a repertory of green catalysts with a potential revenue resource. Biomed Res Int 2013:264020. https://doi.org/10.1155/2013/264020

Priyadharsini P, Dhanasekaran D (2015) Diversity of soil allelopathic Actinobacteria in Tiruchirappalli district, Tamilnadu, India. J Saudi Soc Agric Sci 14(1):54–60. https://doi.org/10.1016/j.jssas.2013.07.001

Radominska-Pandya A, Czernik PJ, Little JM, Battaglia E, Mackenzie PI (1999) Structural and functional studies of UDP-glucuronosyltransferases. Drug Metab Rev 31(4):817–899. https://doi.org/10.1081/DMR-100101944

Regev-Shoshani G, Shoseyov O, Bilkis I, Kerem Z (2003) Glycosylation of resveratrol protects it from enzymic oxidation. Biochem J 374(1):157–163. https://doi.org/10.1042/bj20030141

Remya M, Vijayakumar R (2008) Isolation and characterization of marine antagonistic actinomycetes from west coast of India. Med Biol 15(1):13–19.

925 Ren J, Tang W, Barton CD, Price OM, Mortensen MW, Phillips A, Wald B, Hulme SE,
926 Stanley LP, Hevel J (2022) A highly versatile fungal glucosyltransferase for
927 specific production of quercetin-7-O-β-d-glucoside and quercetin-3-O-β-d-
928 glucoside in different hosts. Appl Microbiol Biotech 106(1):227–245.
929 https://doi.org/10.1007/s00253-021-11716-x
930 Rice-Evans C (2001) Flavonoid antioxidants. Curr Med Chem 8(7):797–807.
931 https://doi.org/10.2174/0929867013373011
932 Ridder L, van der Hooft JJ, Verhoeven S, de Vos RC, van Schaik R, Vervoort J (2012)
933 Substructure-based annotation of high-resolution multistage MSn spectral trees.
934 Rapid Commun Mass Sp 26(20):2461–2471. https://doi.org/10.1002/rcm.6364
935 Romero-Pérez AI, Ibern-Gómez M, Lamuela-Raventós RM, de la Torre-Boronat MC
936 (1999) Piceid, the major resveratrol derivative in grape juices. J Agric Food
937 Chem 47(4):1533–1536. https://doi.org/10.1021/jf981024g
938 Sauer S, Plauth A (2017) Health-beneficial nutraceuticals-myth or reality? Appl
939 Microbiol Biotechnol 101(3):951–961. https://doi.org/10.1007/s00253-016-
940 8068-5
941 Sawada Sy, Suzuki H, Ichimaida F, Yamaguchi M-a, Iwashita T, Fukui Y, Hemmi H,
942 Nishino T, Nakayama T (2005) UDP-glucuronic acid: anthocyanin
943 glucuronosyltransferase from red daisy (*Bellis perennis*) flowers: enzymology
944 and phylogenetics of a novel glucuronosyltransferase involved in flower
945 pigment biosynthesis. J Biol Chem 280(2):899–906.
946 https://doi.org/10.1074/jbc.M410537200

947 Sharipova R, Andreeva O, Strobykina IY, Voloshina A, Strobykina A, Kataev V (2017)
948 Synthesis and antimicrobial activity of glucuronosyl derivatives of
949 steviolbioside from *Stevia rebaudiana*. Chem Nat Compd 53(6):1107–1111.
950 https://doi.org/10.1007/s10600-017-2211-0
951 Shimoda K, Hamada M, Hamada H, Takemoto M, Hamada H (2013) Synthesis of
952 resveratrol glycosides by cultured plant cells. Nat Prod Commun 8(7):907–909.
953 https://doi.org/10.1177/1934578X1300800713
954 Smith MT, Watt JA, Cramond T (1990) Morphine-3-glucuronide-a potent antagonist of
955 morphine analgesia. Life Sci 47(6):579–585. https://doi.org/10.1016/0024-
956 3205(90)90619-3
957 Stachulski A, Jenkins G (1998) The synthesis of O-glucuronides. Nat Prod Rep
958 15(2):173–186.
959 Stachulski AV, Harding JR, Lindon JC, Maggs JL, Park BK, Wilson ID (2006) Acyl
960 glucuronides: biological activity, chemical reactivity, and chemical synthesis. J
961 Med Chem 49(24):6931–6945. https://doi.org/10.1021/jm060599z
962 Sugiura N, Baba Y, Kawaguchi Y, Iwatani T, Suzuki K, Kusakabe T, Yamagishi K,
963 Kimata K, Kakuta Y, Watanabe H (2010) Glucuronyltransferase activity of KfiC
964 from *Escherichia coli* strain K5 requires association of KfiA: KfiC and KfiA
965 are essential enzymes for production of K5 polysaccharide, N-acetylheparosan.
966 J Biol Chem 285(3):1597–1606. https://doi.org/10.1074/jbc.M109.023002
967 Thilakarathna SH, Rupasinghe H (2013) Flavonoid bioavailability and attempts for
968 bioavailability enhancement. Nutrients 5(9):3367–3387.

https://doi.org/10.3390/nu5093367

Thorson JS, Barton WA, Hoffmeister D, Albermann C, Nikolov DB (2004) Structure-based enzyme engineering and its impact on *in vitro* glycorandomization. ChemBioChem 5(1):16–25. https://doi.org/10.1002/cbic.200300620

Thuan NH, Trung NT, Cuong NX, Van Cuong D, Van Quyen D, Malla S (2018) Escherichia coli modular coculture system for resveratrol glucosides production. World J Microb Biot 34(6):1–13. https://doi.org/10.1007/s11274-018-2458-z

Tracy BS, Avci FY, Linhardt RJ, DeAngelis PL (2007) Acceptor specificity of the *Pasteurella hyaluronan* and chondroitin synthases and production of chimeric glycosaminoglycans. J Biol Chem 282(1):337–344. https://doi.org/10.1074/jbc.M607569200

Tsao R (2010) Chemistry and biochemistry of dietary polyphenols. Nutrients 2(12):1231–1246. https://doi.org/10.3390/nu2121231

Uesugi D, Hamada H, Shimoda K, Kubota N, Ozaki S-i, Nagatani N (2017) Synthesis, oxygen radical absorbance capacity, and tyrosinase inhibitory activity of glycosides of resveratrol, pterostilbene, and pinostilbene. Biosci Biotechnol Biochem 81(2):226–230. https://doi.org/10.1080/09168451.2016.1240606

Van der Hooft JJ, de Vos RC, Mihaleva V, Bino RJ, Ridder L, de Roo N, Jacobs DM, van Duynhoven JP, Vervoort J (2012) Structural elucidation and quantification of phenolic conjugates present in human urine after tea intake. Anal Chem 84(16):7263–7271. https://doi.org/10.1021/ac3017339

Wackett L, Gibson D (1982) Metabolism of xenobiotic compounds by enzymes in cell

991 extracts of the fungus *Cunninghamella elegans*. Biochem J 205(1):117–122.
992 https://doi.org/10.1042/bj2050117
993 Wang L-X, Heredia A, Song H, Zhang Z, Yu B, Davis C, Redfield R (2004) Resveratrol
994 glucuronides as the metabolites of resveratrol in humans: characterization,
995 synthesis, and anti-HIV activity. J Pharm Sci 93(10):2448–2457.
996 https://doi.org/10.1002/jps.20156
997 Wang T-T, Deng J-Q, Chen L-Z, Sun L, Wang F-S, Ling P-X, Sheng J-Z (2020) The
998 second member of the bacterial UDP-N-acetyl-D-glucosamine: heparosan
999 alpha-1, 4-N-acetyl-D-glucosaminyltransferase superfamily: GaKfiA from
1000 *Gallibacterium anatis*. Int J Biol Macromol 147:170–176.
1001 https://doi.org/10.1016/j.ijbiomac.2020.01.016
1002 Wang T-T, Zhu C-Y, Zheng S, Meng C-C, Wang T-T, Meng D-H, Li Y-J, Zhu H-M,
1003 Wang F-S, Sheng J-Z (2018) Identification and characterization of a chondroitin
1004 synthase from *Avibacterium paragallinarum*. Appl Microbiol Biotech
1005 102(11):4785–4797. https://doi.org/10.1007/s00253-018-8926-4
1006 Wang Y, Catana F, Yang Y, Roderick R, Van Breemen R (2002) Analysis of resveratrol
1007 in grape products, cranberry juice and wine using liquid chromatography-mass
1008 spectrometry. J Agric Food Chem 50:431–435.
1009 https://doi.org/10.1021/jf010812u
1010 Weymouth-Wilson AC (1997) The role of carbohydrates in biologically active natural
1011 products. Nat Prod Rep 14(2):99–110. https://doi.org/10.1039/NP9971400099
1012 Wilkinson SM, Liew CW, Mackay JP, Salleh HM, Withers SG, McLeod MD (2008)

Escherichia coli glucuronylsynthase: an engineered enzyme for the synthesis of β-glucuronides. Org Lett 10(8):1585–1588. https://doi.org/10.1021/ol8002767

Wilkinson SM, Watson MA, Willis AC, McLeod MD (2011) Experimental and kinetic studies of the *Escherichia coli* glucuronylsynthase: An engineered enzyme for the synthesis of glucuronide conjugates. J Org Chem 76(7):1992–2000. https://doi.org/10.1021/jo101914s

Xu G, Cai W, Gao W, Liu C (2016) A novel glucuronosyltransferase has an unprecedented ability to catalyse continuous two-step glucuronosylation of glycyrrhetinic acid to yield glycyrrhizin. New Phytol 212(1):123–135. https://doi.org/10.1111/nph.14039

Yonekura K, Hanada K (2011) An evolutionary view of functional diversity in family 1 glycosyltransferases. Plant J 66(1):182–193. https://doi.org/10.1111/j.1365-313X.2011.04493.x

Yu C, Shin YG, Chow A, Li Y, Kosmeder JW, Lee YS, Hirschelman WH, Pezzuto JM, Mehta RG, van Breemen RB (2002) Human, rat, and mouse metabolism of resveratrol. Pharm Res 19(12):1907–1914. https://doi.org/10.1023/A:1021414129280

Yu D, Xu F, Zhang S, Shao L, Wang S, Zhan J (2013b) Characterization of a methyltransferase involved in herboxidiene biosynthesis. Bioorg Med Chem Lett 23(20):5667–5670. https://doi.org/10.1016/j.bmcl.2013.08.023

Zakim D, Vessey DA (1974) Membrane dependence of uridine diphosphate glucuronyltransferase: Effect of the membrane on kinetic properties. Biochem

Soc Trans 2(6):1165–1167. https://doi.org/10.1042/bst0021165

Table 1 The glucuronidation (*gca*) gene cluster in *S. chromofuscus* ATCC 49982.

Gene	Size (aa)	Predicted function	Homolog/source/NCBI accession no.	Identity/ Similarity
gcaA	230	TetR family transcriptional regulator	TetR family transcriptional regulator/*Streptomyces* sp. CRXT-G-22]/WP_187751940.1	71%/81%
gcaB	484	UDP-Glucose dehydrogenase	UDP-glucose/GDP-mannose dehydrogenase family protein/ *Streptomyces* sp. SolWspMP-5a-2 /WP_093832645.1	82%/86%
gcaC	402	UDP-Glucuronyltransferase	UDP-glucuronyl/UDP-glucosyltransferase/*Streptomyces malaysiensis*/NIY63294.1	70%/80%
gcaD	320	UDP-Glucose pyrophosphorylase	GalU/*Streptococcus pneumonia*/AJ004869.1	45%/62%
gcaE	540	MFS transporter	MFS transporter/*Streptomyces hygroscopicus*/WP_060945424.1	83%/90%

Figure legends

Fig. 1 Screening of five actinomycete strains for the ability to biotransform resveratrol. **a** HPLC analysis (300 nm) of biotransformation of resveratrol by five actinomycete strains. (i) resveratrol + YM medium; (ii) resveratrol + *S. roseum* No. 79089; (iii) resveratrol + *S. reseiscleroticus* ATCC 53903; (iv) resveratrol + A. *hibisca* P157-2; (v) resveratrol + *Streptomyces* sp. FERM BP-2474; (vi) resveratrol + *S. chromofuscus* ATCC 49982. **b** UV spectra comparison of the substrate and product **1**. **c** UV spectra comparison of the substrate and product **2**. **d** ESI-MS (-) spectrum of product **1**. **e** ESI-MS (-) spectrum of product **2**.

Fig. 2 Key HMBC correlations of **1**-**7**.

Fig. 3 HPLC analysis of glucuronidation of different substrates by *S. chromofuscus* ATCC 49982. **a** Glucuronidation of quercetin (350 nm); **b** Glucuronidation of ferulic acid (300 nm); **c** Glucuronidation of vanillic acid (300 nm). (i) substrate + YM medium; (ii) substrate + *S. chromofuscus* ATCC 49982.

Fig. 4 A putative glucuronidation (*gca*) gene cluster discovered in *S. chromofuscus* ATCC 49982. **a** Organization of the *gca* gene cluster. **b** Proposed pathways for UDP-glucuronic acid biosynthesis and glucuronidation of resveratrol.

Fig. 5 Heterologous expression and *in vitro* functional characterization of GcaC. **a** SDS-PAGE analysis of the purified recombinant GcaC from E. coli BL21(DE3). Lane 1: Purified GcaC; Lane 2: Protein ladder. **b** HPLC analysis (300 nm) of the *in vitro* reaction of GcaC with resveratrol. (i) resveratrol + reaction buffer without GcaC; (ii) resveratrol + GcaC. **c** ESI-MS (-) spectrum of *in vitro* product **1**. **d** ESI-MS (-) spectrum

of *in vitro* product **2**.

Fig. 6 HPLC analysis of *in vitro* glucuronidation of different sugar acceptor substrates by GcaC. **a** Glucuronidation of quercetin (350 nm); **b** Glucuronidation of ferulic acid (300 nm); **c** Glucuronidation of vanillic acid (300 nm). **d** Glucuronidation of curcumin (420 nm); **e** Glucuronidation of vanillin (300 nm); **f** Glucuronidation of chrysin (350 nm); **g** Glucuronidation of zearalenone (250 nm); **h** Glucuronidation of apigenin (350 nm). (i) substrate incubated with the reaction buffer without GcaC; (ii) substrate incubated with the reaction buffer with GcaC.

Fig. 7 Determination of the optimum *in vitro* reaction conditions for GcaC. **a** Effect of reaction temperature on the GcaC glucuronidation activity. **b** Effect of reaction pH on the GcaC glucuronidation activity. **c** Effect of metal ions on the GcaC glucuronidation activity. Data are presented as the mean ± SD from three independent experiments.

Fig. 8 Optimization of *in vivo* production of resveratrol glucuronides by *E. coli* BL21(DE3)/pJR36. **a** HPLC analysis (300 nm) of resveratrol glucuronidation by GcaC in *E. coli* BL21(DE3). (i) Commercial standard of resveratrol; (ii) resveratrol + *E. coli* BL21(DE3)/pET28a; (iii) resveratrol + *E. coli* BL21(DE3)/pJR36. **b** Effect of cell density on resveratrol glucuronidation **c** Effect of reaction pH on resveratrol glucuronidation by *E. coli* BL21(DE3)/pJR36. **d** Effect of temperature on resveratrol glucuronidation by *E. coli* BL21(DE3)/pJR36. **e** Effect of reaction time on resveratrol glucuronidation by *E. coli* BL21(DE3)/pJR36. **f** Effect of substrate concentration on resveratrol glucuronidation by *E. coli* BL21(DE3)/pJR36. Data are presented as the mean ± SD from three independent experiments.

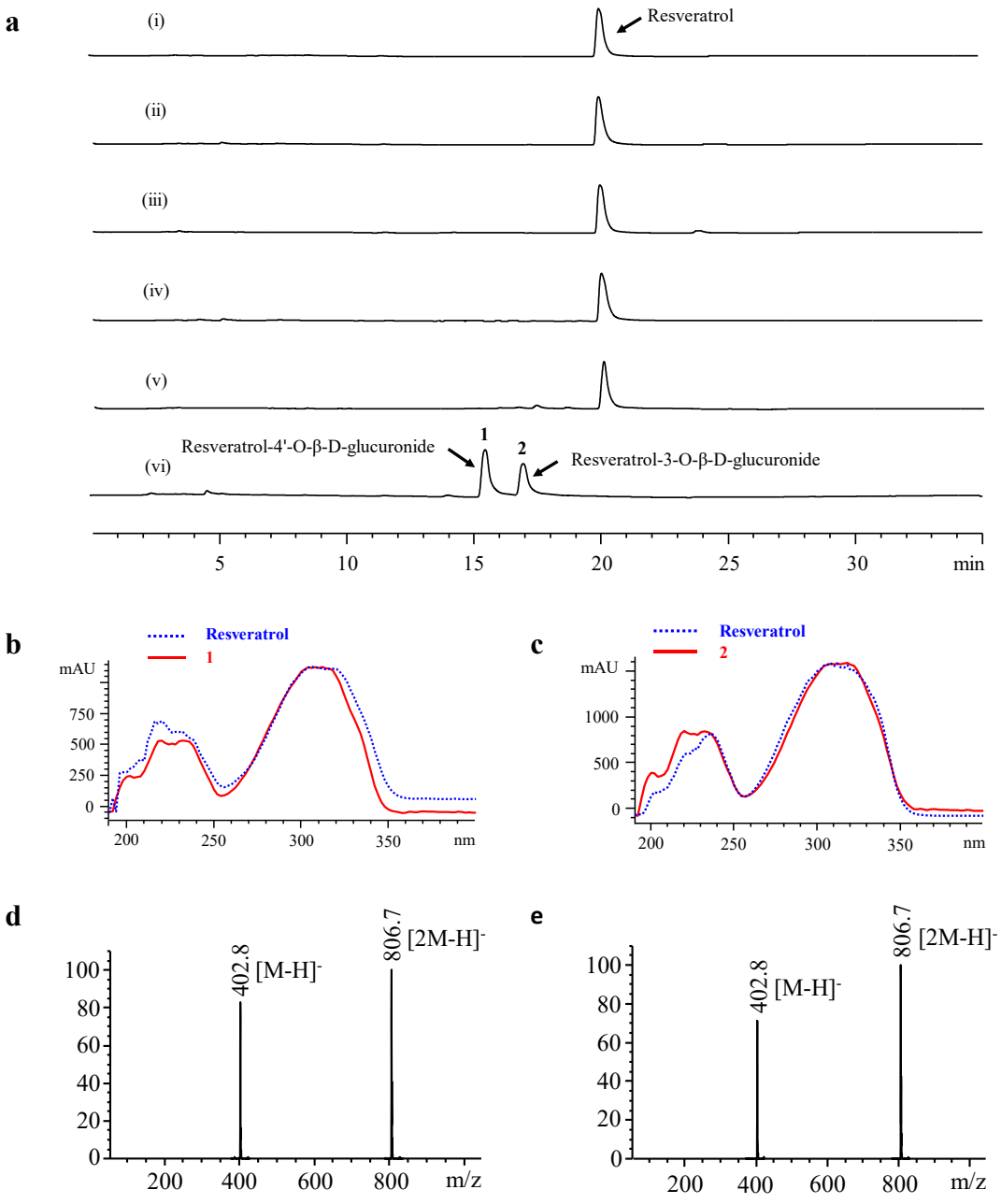
a
(i)
Resveratrol
(ii)
(iii)
(iv)
(v)
(vi)
Resveratrol-4'-O-β-D-glucuronide
1
2
Resveratrol-3-O-β-D-glucuronide
5
10
15
20
25
30
min
b
Resveratrol
1
mAU
750
500
250
0
200
250
300
350
nm
c
Resveratrol
2
mAU
1000
500
0
200
250
300
350
nm
d
402.8
[M-H]-
806.7
[2M-H]-
100
80
60
40
20
0
200
400
600
800
m/z
e
402.8
[M-H]-
806.7
[2M-H]-
100
80
60
40
20
0
200
400
600
800
m/z

Fig. 1

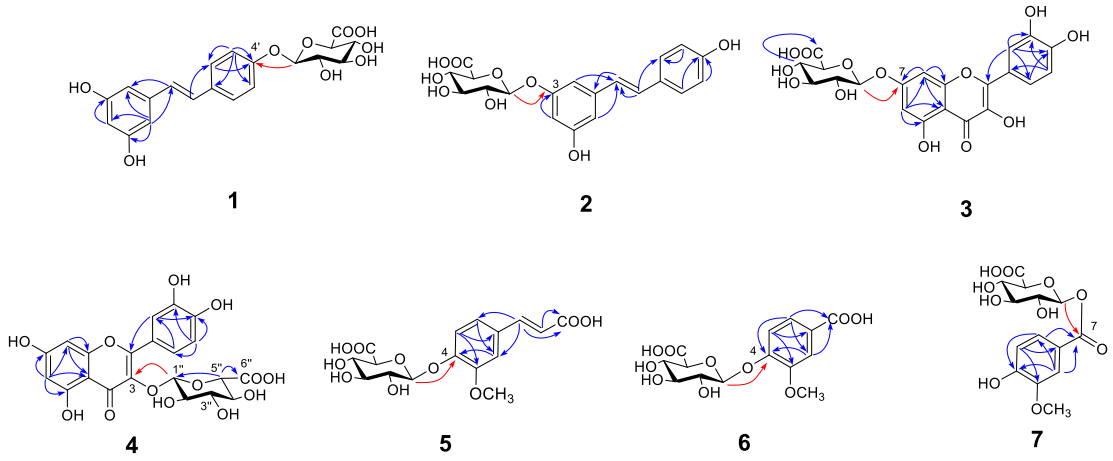

Fig. 2

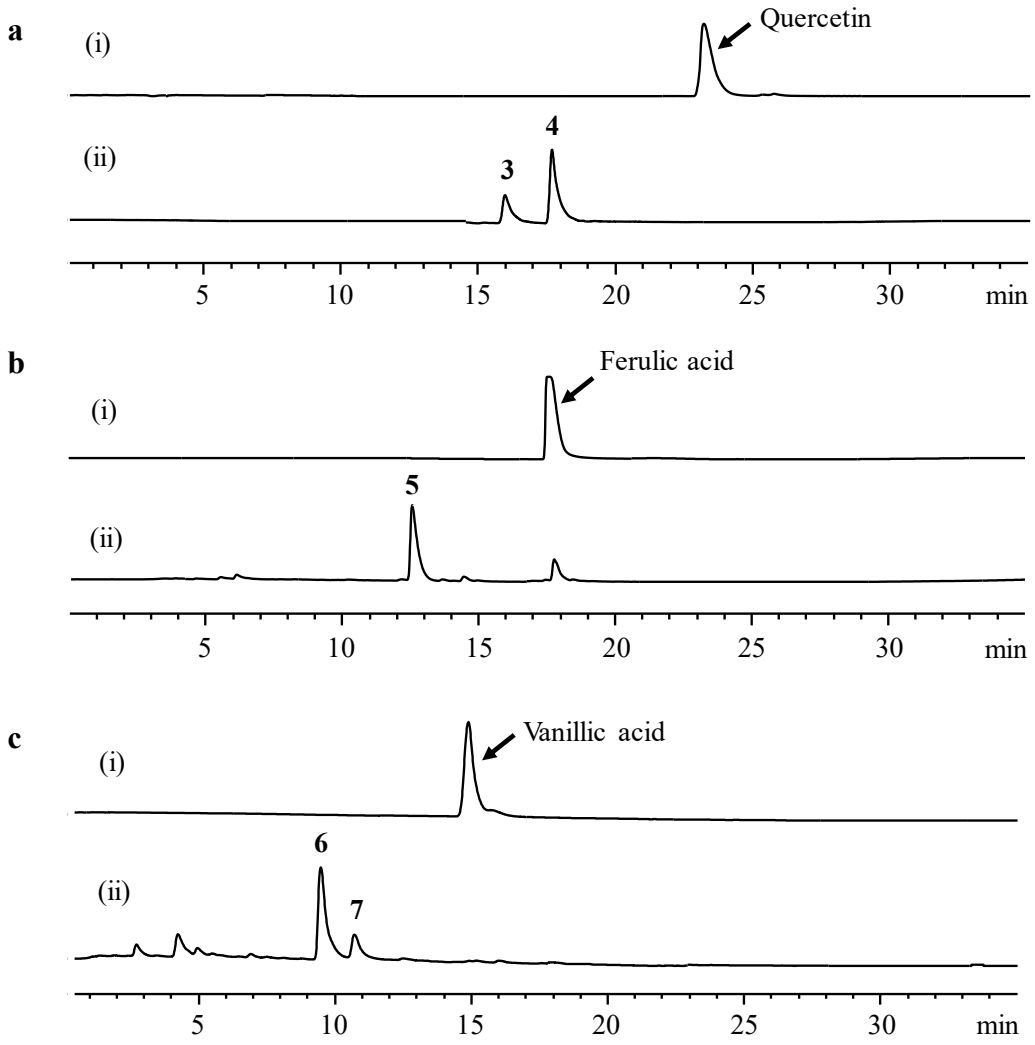
a
(i)
Quercetin
(ii)
3
4
5
10
15
20
25
30
min
b
(i)
Ferulic acid
(ii)
5
10
15
20
25
30
min
c
(i)
Vanillic acid
(ii)
6
7
5
10
15
20
25
30
min

Fig. 3

a


gcaA
gcaB
gcaC
gcaD
gcaE

b

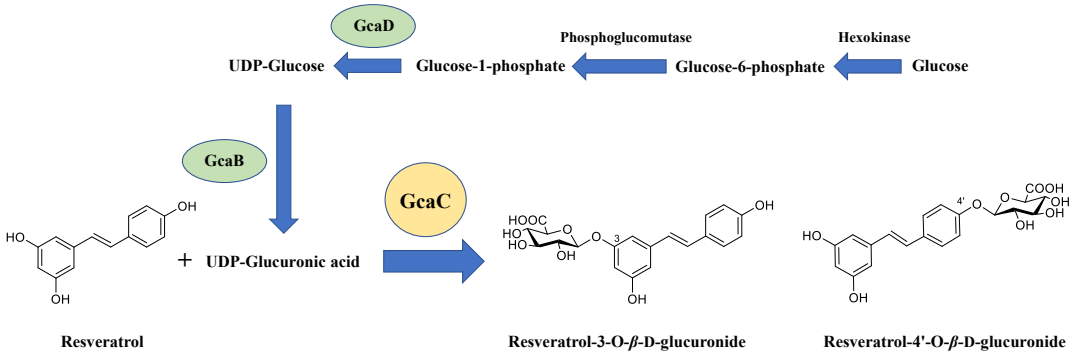
GcaD
UDP-Glucose
Glucose-1-phosphate
Phosphoglucomutase
Glucose-6-phosphate
Hexokinase
Glucose
GcaB
GcaC
UDP-Glucuronic acid
Resveratrol
Resveratrol-3-O-β-D-glucuronide
Resveratrol-4'-O-β-D-glucuronide

Fig. 4

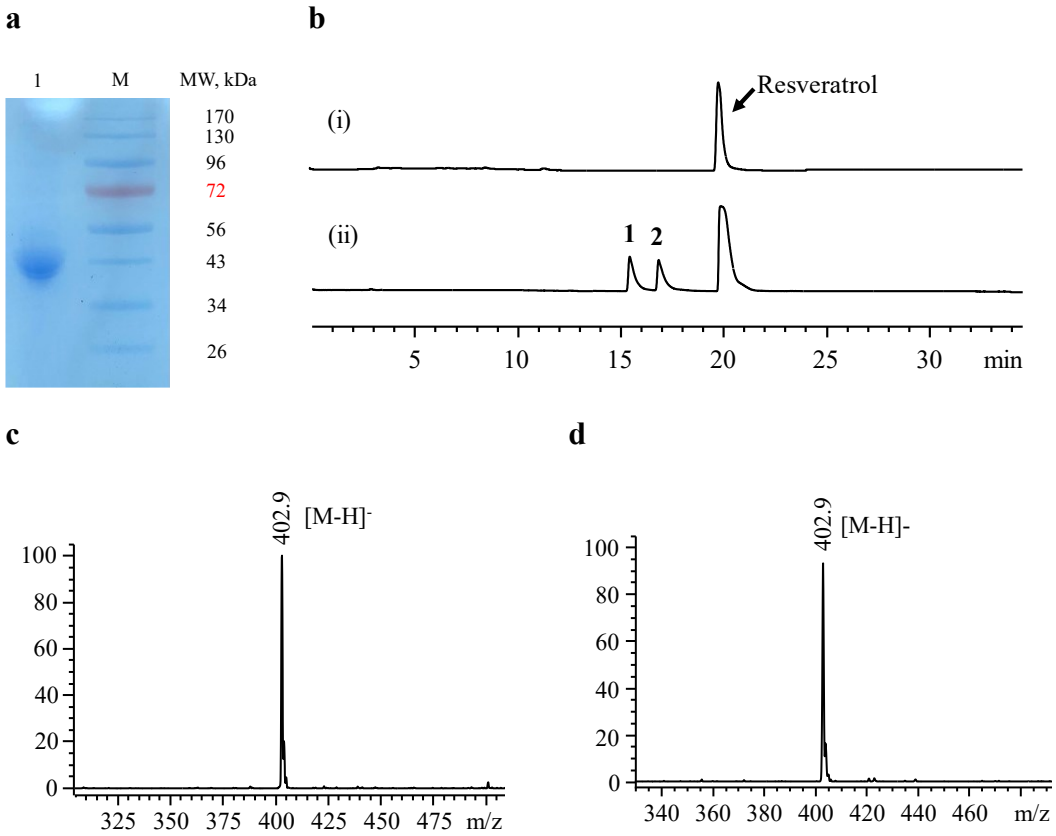
a
1
M
MW, kDa
170
130
96
72
56
43
34
26
b
(i)
Resveratrol
(ii)
1
2
5
10
15
20
25
30
min
c
402.9
[M-H]-
100
80
60
40
20
0
325
350
375
400
425
450
475
m/z
d
402.9
[M-H]-
100
80
60
40
20
0
340
360
380
400
420
440
460
m/z

Fig. 5

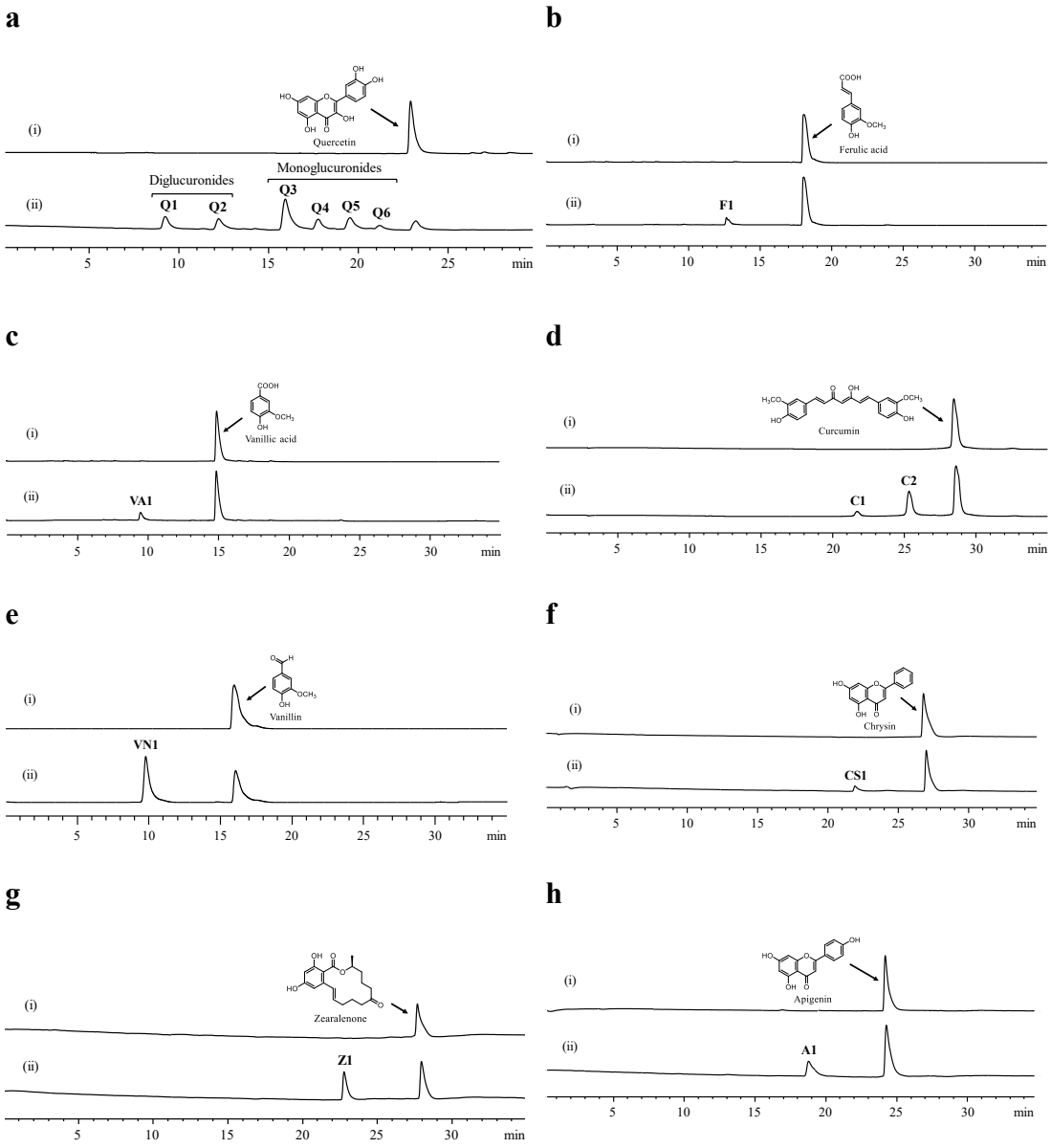
a
(i)
Quercetin
Diglucuronides
Monoglucuronides
(ii)
Q1
Q2
Q3
Q4
Q5
Q6
5
10
15
20
25
min
b
(i)
Ferulic acid
(ii)
F1
5
10
15
20
25
30
min
c
(i)
Vanillic acid
(ii)
VA1
5
10
15
20
25
30
min
d
(i)
Curcumin
(ii)
C1
C2
5
10
15
20
25
30
min
e
(i)
Vanillin
(ii)
VN1
5
10
15
20
25
30
min
f
(i)
Chrysin
(ii)
CS1
5
10
15
20
25
30
min
g
(i)
Zearalenone
(ii)
Z1
5
10
15
20
25
30
min
h
(i)
Apigenin
(ii)
A1
5
10
15
20
25
30
min

Fig. 6

1189

1190

1191

a

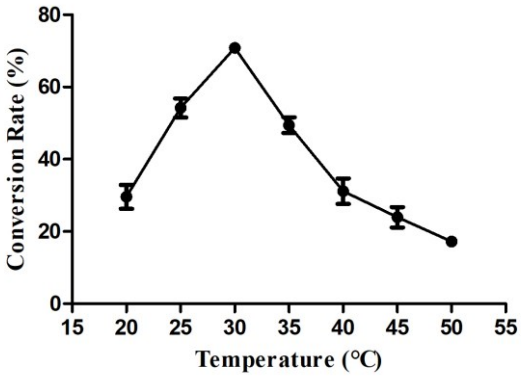

b

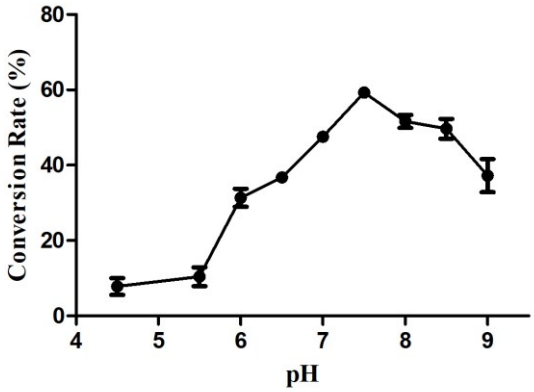

c

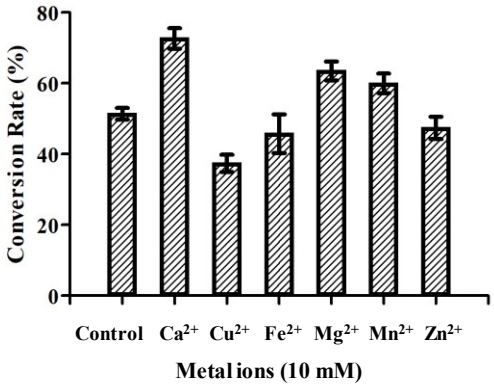

1192 **Fig. 7**

1193

1194

1195

1196

1197

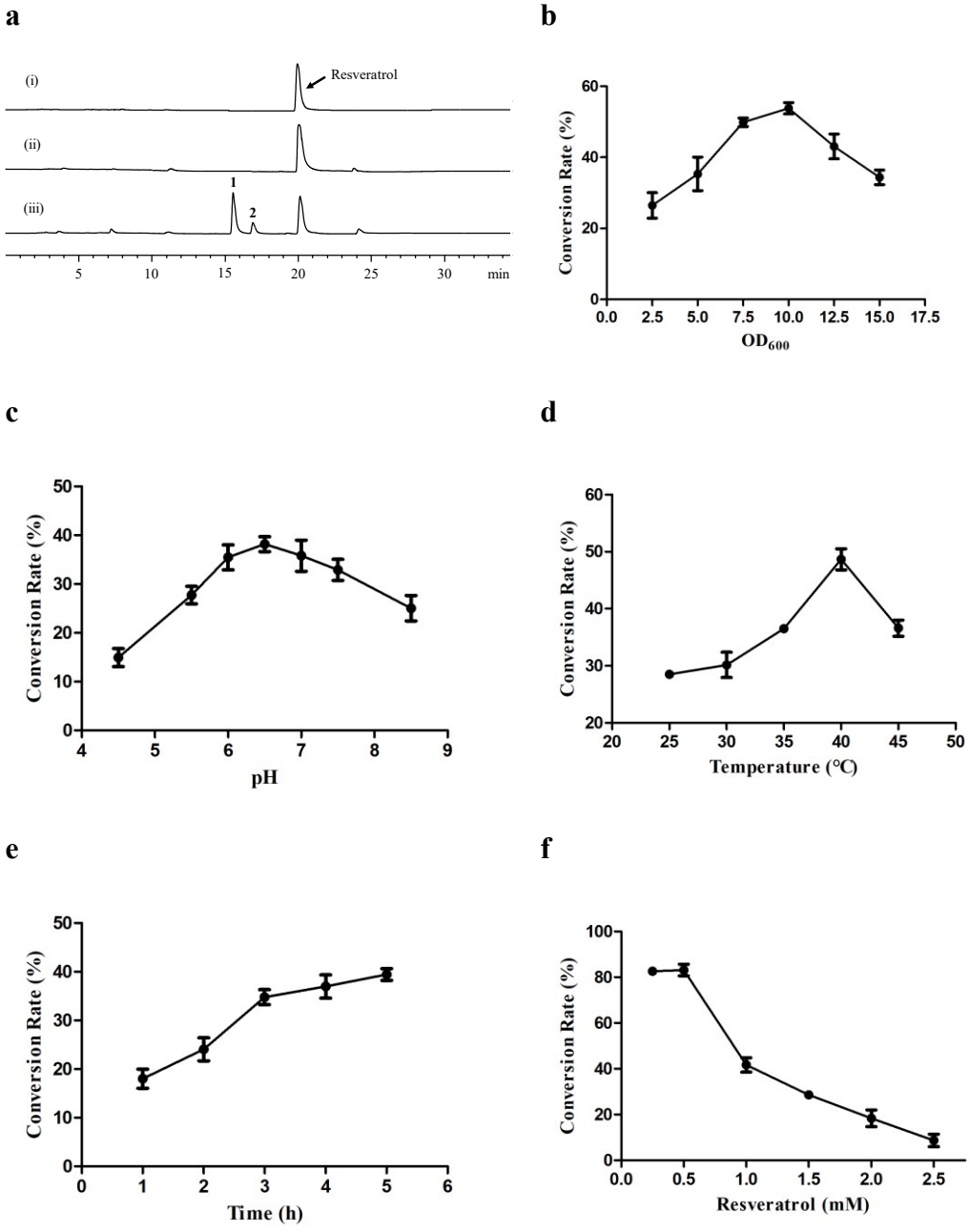

1198 **Fig. 8**

1199

1200

1201